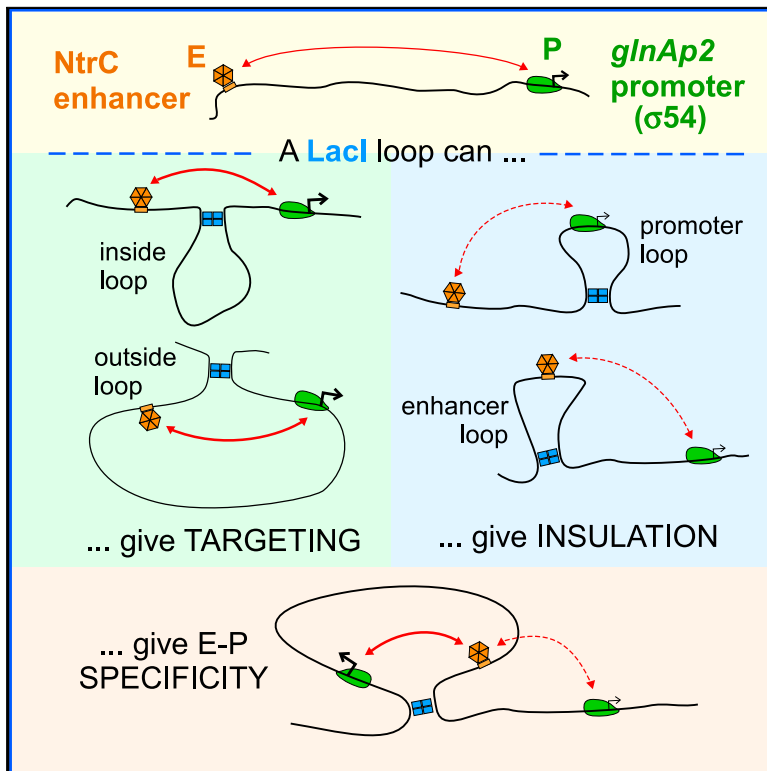


## Positive and Negative Control of Enhancer-Promoter Interactions by Other DNA Loops Generates Specificity and Tunability

### Graphical Abstract



### Authors

Nan Hao, Keith E. Shearwin, Ian B. Dodd

### Correspondence

ian.dodd@adelaide.edu.au

### In Brief

Eukaryotic enhancers contact their promoters within a network of DNA loops. Hao et al. used the *E. coli* NtrC system and modeling to measure how DNA loops formed by LacI affect enhancer action, showing strong positive or negative effects able to provide control of promoter specificity.

### Highlights

- Effect of DNA distance on NtrC enhancer action implies weak looping to the promoter
- A LacI DNA loop can target the enhancer to the promoter or cause insulation
- A single LacI loop can combine targeting and insulation to give promoter specificity
- Modeling shows sensitivity of enhancer action to control by other loops is tunable



# Positive and Negative Control of Enhancer-Promoter Interactions by Other DNA Loops Generates Specificity and Tunability

Nan Hao,<sup>1,2</sup> Keith E. Shearwin,<sup>1</sup> and Ian B. Dodd<sup>1,3,\*</sup>

<sup>1</sup>Department of Molecular and Biomedical Science, The University of Adelaide, Adelaide, SA 5005, Australia

<sup>2</sup>CSIRO Synthetic Biology Future Science Platform, Canberra, ACT 2601, Australia

<sup>3</sup>Lead Contact

\*Correspondence: [ian.dodd@adelaide.edu.au](mailto:ian.dodd@adelaide.edu.au)

<https://doi.org/10.1016/j.celrep.2019.02.002>

## SUMMARY

Enhancers are ubiquitous and critical gene-regulatory elements. However, quantitative understanding of the role of DNA looping in the regulation of enhancer action and specificity is limited. We used the *Escherichia coli* NtrC enhancer- $\sigma$ 54 promoter system as an *in vivo* model, finding that NtrC activation is highly sensitive to the enhancer-promoter (E-P) distance in the 300–6,000 bp range. DNA loops formed by Lac repressor were able to strongly regulate enhancer action either positively or negatively, recapitulating promoter targeting and insulation. A single LacI loop combining targeting and insulation produced a strong shift in specificity for enhancer choice between two  $\sigma$ 54 promoters. A combined kinetic-thermodynamic model was used to quantify the effect of DNA-looping interactions on promoter activity and revealed that sensitivity to E-P distance and to control by other loops is itself dependent on enhancer and promoter parameters that may be subject to regulation.

## INTRODUCTION

Enhancers are gene-regulatory elements that bind transcription factors and can activate transcription when located far upstream or downstream of the promoter (Furlong and Levine, 2018; Long et al., 2016; Spitz, 2016; Zabidi and Stark, 2016). Activation requires enhancer-promoter (E-P) contact, and because enhancers act primarily on promoters in *cis*, DNA loops are formed. Action in *cis* is favored because the intervening DNA acts as a tether that holds the enhancer and promoter near to each other. Enhancers are ubiquitous and important, far outnumbering genes in eukaryotic genomes (Dunham et al., 2012; Kvon et al., 2014), with enhancer dysfunction increasingly recognized as a cause of genetic diseases (Mumbach et al., 2017; Spitz, 2016).

Genome-wide surveys reveal complex and specific long-range E-P interactions, often occurring over large genomic distances and always within the context of other DNA-looping interactions (Kieffer-Kwon et al., 2013; Mumbach et al., 2017; Rao

et al., 2014). Some enhancers contact multiple promoters, and some promoters are contacted by multiple enhancers. Questions of how promoter activation by enhancers can be efficient and specific and how activation is shared between multiple enhancers and promoters remain to be answered.

Although some E-P specificity is provided by the factors bound at the promoter or enhancer (Zabidi and Stark, 2016), it is clear that enhancer action can be strongly regulated by other DNA looping elements in the tether that assist or interfere with E-P looping. Contact between specific E-P pairs can be stimulated by interaction between natural or artificial DNA elements near the promoter and enhancer that brings the enhancer and promoter closer together, termed E-P targeting (Deng et al., 2014; Priest et al., 2014a; Zabidi and Stark, 2016). Conversely, inhibition of specific E-P contacts occurs when a site within the E-P tether forms a loop to a site outside the tether, with the resulting loop around the enhancer or promoter somehow isolating them from each other, termed E-P insulation (Bondarenko et al., 2003; Chetverina et al., 2014; Priest et al., 2014a). Pervasive DNA loops formed by CTCF binding sites in mammals and other insulator elements in *Drosophila* partition genomes into large domains, where contact between sites within the same domain is favored over contact with sites in different domains (Dixon et al., 2012; Rao et al., 2014; Sexton et al., 2012).

Sharing of activation between multiple enhancers and promoters is also a question of DNA looping, in this case whether a specific E-P interaction is diminished by alternative DNA loops formed by the enhancer or promoter (Long et al., 2016). What controls the outcome of these interactions is unclear. Competition between multiple promoters for activation by a shared enhancer (Cho et al., 2018; Deng et al., 2014; Fukaya et al., 2016) implies that the alternative enhancer interactions can be inhibitory, while the ability of multiple enhancers to work additively at a promoter (Bothma et al., 2015) implies that alternative interactions can be stimulatory.

The importance and complexity of these long-range looping interactions underscores the need for a theoretical framework to help decipher genomic design principles. Our approach has been to combine experiments and modeling using highly defined looping systems in *E. coli* cells, allowing measurement of absolute looping efficiencies, and quantitation of stimulatory or inhibitory interactions between pairs of DNA loops (Hao et al., 2017a; Priest et al., 2014a, 2014b). These analyses used



long-range repressive systems; here we extend these studies to long-range activation.

Activation of  $\sigma 54$ -dependent promoters in bacteria displays similarities to enhancer action in eukaryotes (Bush and Dixon, 2012; Zhang et al., 2016) and provides a simple model system for enhancer regulation by DNA looping. First, unlike the major  $\sigma 70$ -containing RNAP in bacteria but similar to eukaryotic RNAPs,  $\sigma 54$ -RNAP cannot by itself progress beyond the closed complex at the promoter. Second, conversion to the initiation competent complex requires catalytic intervention using the energy of ATP hydrolysis. This is achieved in the  $\sigma 54$ -RNAP case by a class of activators termed bacterial enhancer binding proteins (bEBPs), which interact with the  $\sigma 54$ -RNAP closed complex and convert it to the open complex. Third, the bacterial activator proteins assemble into enhanceosome-like multimeric complexes at clusters of binding sites that, although usually located about 100 bp upstream of the promoter, can also function when moved a few thousand base pairs upstream or downstream of the promoter (Hao et al., 2017b; Reitzer and Magasanik, 1986). Fourth, the bEBP-bound enhancer and the promoter interact by DNA looping, as observed by electron and scanning force microscopy (Rippe et al., 1997; Su et al., 1990), but like eukaryotic enhancers, activation can also occur when the promoter and the enhancer are on separate but interlinked DNA circles (Dunaway and Dröge, 1989; Wedel et al., 1990). Thus, the role of the DNA tether linking the enhancer and promoter is to hold the two sites at a high relative concentration. Studies focused on bacterial E-P distances less than 500 bp have shown that activation is sensitive to factors that alter this relative concentration, such as tether length, intrinsic curvature, and the binding of proteins that bend or stiffen the DNA (Amit et al., 2011; Schulz et al., 2000).

To quantify control of E-P looping *in vivo*, we analyzed activation of the *E. coli glnAp2* promoter by the bEBP protein NtrC (Friedman and Gelles, 2012; Ninfa et al., 1987; Reitzer and Magasanik, 1986; Sasse-Dwight and Gralla, 1988) using chromosomal reporters and a simple combined thermodynamic-kinetic model. Systematic measurements of the decrease in activation as the E-P spacing was increased from 300 to 6,000 bp imply weak looping in this system. We saw strong positive or negative effects on E-P looping by a variety of DNA loops formed by the Lac repressor (LacI) and showed that combining these effects can produce a large change in promoter specificity. Competition between two promoters for a single enhancer was weak, consistent with weak looping. Modeling indicates that variation of the thermodynamic and kinetic parameters of the enhancer and promoter can alter the sensitivity to DNA distance and to control by other loops, arguing that enhancers and promoters may be heterogeneous in their response to regulation by DNA loops.

## RESULTS

### Enhancer Action as a Function of Distance

Beyond 300 bp, the efficiency of DNA looping decreases with increasing DNA distance between the interacting sites (Hao et al., 2017a; Priest et al., 2014b). We thus expected that the relationship between promoter activity and E-P distance would be revealing about the role of E-P looping in activation. Here,

and throughout the paper, we used a minimal NtrC E-P system (Figure 1A; Amit et al., 2011; Hao et al., 2017b), comprising the *E. coli glnAp2* promoter and its two strong NtrC binding sites (Ninfa et al., 1987; Reitzer and Magasanik, 1986; Sasse-Dwight and Gralla, 1988). NtrC was supplied from the endogenous locus (*glnG*) and was activated by constitutive phosphorylation by NtrB (encoded by *glnL*) by using the *glnL*:A129T mutation, which reduces phosphatase activity (Pioszak and Ninfa, 2003). We showed previously that promoter activity in this system fell as the E-P distance ( $d$ ) was increased from 300 to 11,700 bp (Hao et al., 2017b), and we here collected more data in the 300–6,000 bp range (Figures 1A and 1B).

The promoter was placed upstream of a *lacZ* reporter gene in the *E. coli* chromosome, with the enhancer further upstream in most constructs (Figure 1A). Maximal enhancer-dependent activity was 0.063 transcripts  $s^{-1}$  at the 300 bp E-P spacing (16 s per initiation; STAR Methods), decreasing steadily to approximately 11-fold lower activity at 6,000 bp (Figure 1B). The activity of the construct with the enhancer downstream was equivalent to its upstream counterparts (Figure 1B, green point). To better understand the relationship between DNA looping and enhancer activity, we developed a combined thermodynamic and kinetic model.

The probability of DNA looping between two protein-bound sites on the same DNA is a balance of the energetic cost and benefit of looping. The cost of looping is inversely related to the effective concentration of one DNA site relative to another site on the same DNA,  $J$  (Figure 1C). The decrease in  $J$  with increasing  $d$  beyond 300 bp is due to the increasing entropic cost of bringing the sites together. Previous measurements of  $J$  from LacI looping (Hao et al., 2017a; Priest et al., 2014b) provide the relationship between  $J$  and  $d$  on the *E. coli* chromosome (Figures 1C and S2A; STAR Methods).

The energetic benefit is due to the interaction between the proteins binding to each site (Figure 1D) and can be represented by the factor  $I$  (Figure 1D; Hao et al., 2017a).  $I$  is inversely related to the benefit of looping, with lower  $I$  values representing a stronger interaction.  $I$  has units of concentration, akin to a dissociation constant. The value of  $I$  is dependent on the specific looping proteins, their concentrations, and their binding sites (Hao et al., 2017a) and is unknown for the NtrC-*glnAp2* system.

The balance of this cost and benefit is given by the ratio  $J/I$ , which is the probability of the looped state relative to the unlooped state, giving the fractional looping,  $F$ , as  $J/(J + I)$  (Figure 1DE; Hao et al., 2017a; see also Amit et al., 2011). The value of  $I$  thus determines how  $F$  for sites on the *E. coli* chromosome falls as  $d$  is increased (Figure 1E). With low  $I$  values, looping is strong and falls slowly with  $d$ ; with high  $I$  values, looping is weak and falls rapidly with  $d$ .

To understand how  $F$  in turn affects promoter activity, the reactions at the promoter need to be considered. We used a kinetic model that is similar to previous schemes for  $\sigma 54$  promoters (Friedman and Gelles, 2012; Ninfa et al., 1987; Sasse-Dwight and Gralla, 1988; Schulz et al., 2000) and that specifies three states of the promoter: free, bound by  $\sigma 54$ -RNAP in a closed complex, and bound by  $\sigma 54$ -RNAP in an open complex (Figure 1F). The activity of the promoter is determined by four reaction rates (Figure 1F):  $k_c$  and  $k_u$  for RNAP binding and

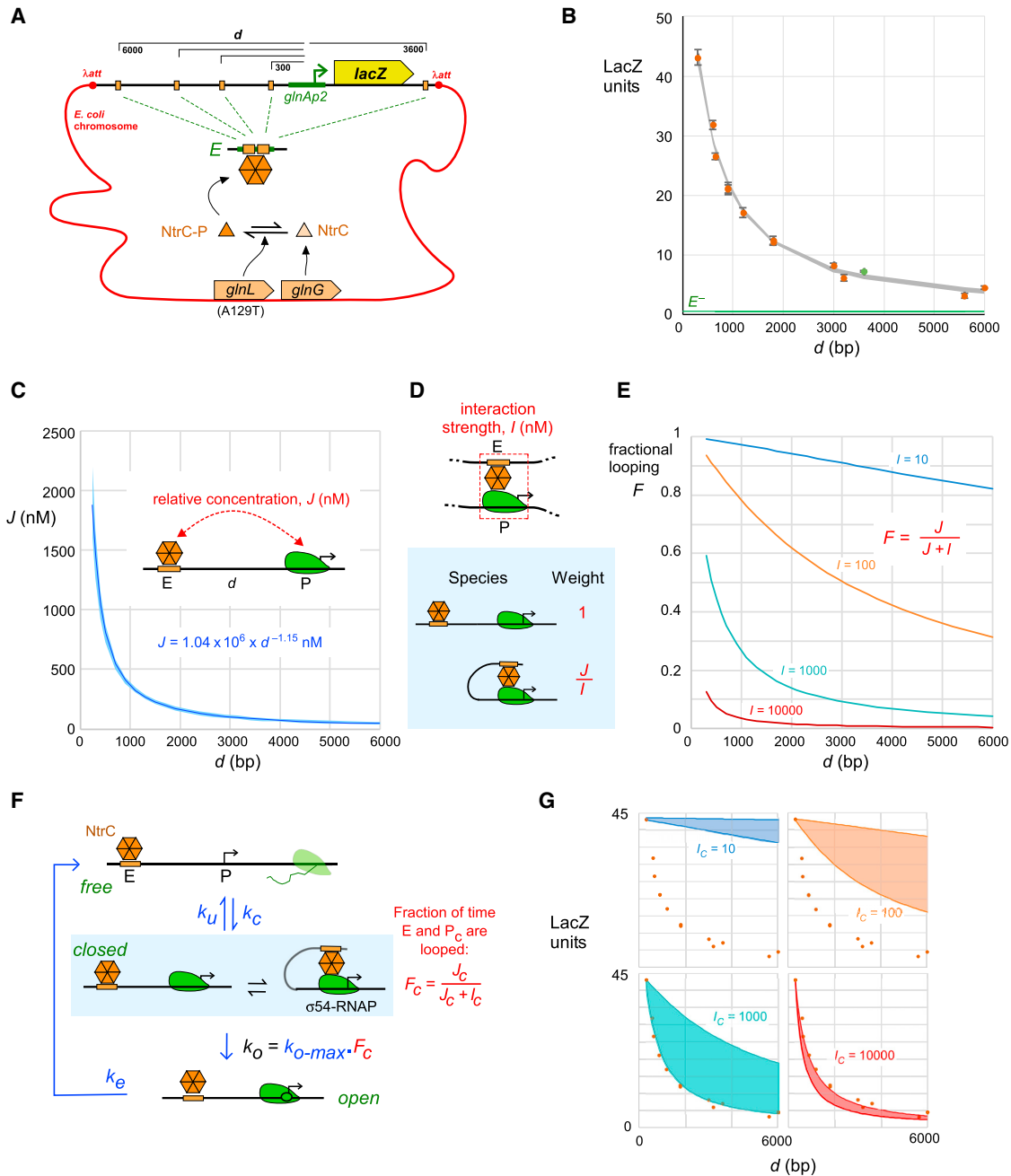


**Figure 1. Enhancer Action as a Function of DNA Distance**

(A) System for measurement of NtrC enhancer action and the effect of distance from the promoter (see STAR Methods and Figure S1 for cloning details).  
 (B) Points are measured promoter activity versus E-P distance. The green point is with the enhancer downstream of the promoter. Errors are 95% confidence limits of repeated assays (Student's t test,  $n = 9$ ). Green lines show activity in the absence of the enhancer. The gray area shows the range of activities obtained by model fitting.  
 (C) The blue area shows the range of fitted power-law relationships between  $J$  (the relative concentration of sites on the same DNA) and DNA distance,  $d$ , obtained from previous measurements of  $J$  for LacI loop-dependent repression (Hao et al., 2017a; Priest et al., 2014a, 2014b). See STAR Methods and Figure S2A. The average power law relating  $J$  and  $d$  is shown.  
 (D)  $I$  quantitates the interaction strength of protein-bound DNA sites, with looping propensity given by the ratio of  $J$  and  $I$  (see text).  
 (E) Plot of the fractional looping  $F$  versus  $d$  for different  $I$  values, calculated using the  $J$  versus  $d$  relationship (C) and the inset equation (Hao et al., 2017a).  
 (F) Schematic of the kinetic model. See main text.  
 (G) Selected plots of activity versus distance for different  $I_C$ . Each plot has different values of  $k_C$ ,  $k_U$ ,  $k_{O-max}$ , and  $k_E$  that were able to give  $A = 43.1$  units at 300 bp. The upper and lower plots in each panel are the extremes of the E-P variants for that  $I_C$  and maximal allowed rates of  $1 \text{ s}^{-1}$  for  $k_C$ ,  $k_{O-max}$ , and  $k_E$ . Points are from (B).

unbinding,  $k_o$  for the closed  $\rightarrow$  open complex transition, and  $k_e$  for initiation and escape. The promoter activity can be calculated for any combination of values of these four rates (Figure S2C; STAR Methods).

In the model, DNA looping controls promoter activity by affecting  $k_o$ . Specifically, the model assumes that the closed  $\rightarrow$  open rate is proportional to the fraction of time,  $F_C$ , that the closed complex (Pc) spends looped to the enhancer (Figure 1F).  $k_o$  thus varies from zero in the absence of the enhancer to a maximal value,  $k_{o-max}$ , in the case of full looping.  $F_C$  is a function of  $J_C$  (dependent on the E-Pc tether) and  $I_C$  for the E-Pc interaction (dependent on enhancer occupancy by NtrC and the strength of the biochemical interaction between the NtrC multimer and the open complex; Figure S2B; STAR Methods). Our model differs from those of Amit et al. (2011) and Bothma et al. (2015) in that promoter activity is not necessarily proportional to the fraction of looping, as kinetic steps apart from the closed  $\rightarrow$  open step can be rate limiting.

The model was able to closely match the activity versus  $d$  data (Figure 1B, gray area; STAR Methods) with E-P variants displaying large ranges and combinations of values for the four reaction rates  $k_c$ ,  $k_u$ ,  $k_{o-max}$ , and  $k_e$ . However the  $I_C$  values were constrained between about 1,000 and 10,000 nM. In comparison, we have estimated much stronger  $J$  values of <100 nM for looping by LacI and  $\lambda$  CI (Hao et al., 2017a). Many E-P variants gave promoters dominated by the closed complex, consistent with *in vivo* footprinting results (Sasse-Dwight and Gralla, 1988).

The constraints on  $I_C$  occur because it is the primary determinant of the fall in enhancer activity in response to increasing  $d$ , through its effect on  $F_C$  (Figure 1F). Low  $I_C$  values make promoter activity relatively insensitive to  $d$ , and high  $I_C$  values make activity  $d$  sensitive (Figure 1G). Distance sensitivity is also affected by the kinetic parameters, giving some variation within the  $I_C$  window.  $d$  sensitivity is maximal when  $k_o$  is rate limiting and loop-dependent changes in  $k_o$  strongly affect initiation rate;  $d$  sensitivity is minimal when the  $k_c$  or  $k_e$  steps are limiting and  $k_o$  has little impact on initiation. Even with kinetic parameters that maximize  $d$  sensitivity,  $I_C$  values between 1,000 and 10,000 nM are needed to optimally reproduce the observed strong  $d$  sensitivity (Figure 1G), indicating weak E-P looping in the NtrC-*glnAp2* system.

This basic model for the NtrC-*glnAp2* system allowed us to quantitate how E-P looping and activation can be controlled by DNA loops of various geometries formed by a separate protein.

### Stimulation of Enhancer Action by Inside Loop Assistance

We previously developed a theoretical framework for loop interactions to analyze interactions between LacI or  $\lambda$  CI loops (Hao et al., 2017a; Priest et al., 2014a). Here, we combined this approach with our NtrC-*glnAp2* model.

When DNA looping elements are placed internal to two sites, the interaction of the sites increases. This loop assistance can be rationalized by the internal loop effectively shortening the distance between the sites, thus increasing  $J$  (Figure 2A; Doyle et al., 2014; Priest et al., 2014a). We previously introduced the term  $\alpha$  to quantitate the magnitude of this change in  $J$  when the internal loop is fully formed (Priest et al., 2014a; Figure S2B; STAR Methods), with loop assistance being the case when  $\alpha > 1$

(Figure 2A). For reasonably long DNA segments, we expect  $\alpha$  to be independent of the looping elements.  $\alpha$  thus provides a measure of how DNA and site geometry affects loop interactions, which we expect will be necessary to understand regulation by other loops.

Previously, we showed that *glnAp2* activity with an E-P distance of 12 kb was moderately increased by internal DNA loops formed by dimeric dCas9 proteins (Hao et al., 2017b). To better quantitate loop assistance, we used the better characterized LacI protein to form the internal loop (Figure 2B). The E-P distance was about 20 kb, at which activity was barely above the  $E^-$  background (Figure 2B). However, with a pair of strong LacI binding sites (Oid and O1) nested 500 bp internally to the E-P loop, a strong loop assistance effect was seen, with enhancer-dependent activity increased about 5-fold (Figure 2B). Shortening the internal E-Oid and O1-P arms to 300 bp increased the regulatory effect to about 10-fold.

Estimates for  $\alpha$  can be obtained from the promoter activities in the absence and presence of LacI looping, taking into account how often we expect the assisting loop to form (STAR Methods; Figure S3). For this we use our measured  $J$  value of 35 nM for LacI Oid-O1 (Hao et al., 2017a) and the expected  $J$  for the LacI loop on the basis of the  $J$ -versus- $d$  relationship. The  $\alpha$  values calculated from the data in Figure 2B indicate that the internal LacI loop strongly increases  $J$  for the E-P loop, by about 16- or 40-fold. Note that the fold effect of the assisting loop on overall activity is less than  $\alpha$ , in part because the LacI loop does not form 100% of the time (we expect only 24% LacI looping alone at these distances) and in part because promoter activity does not rise proportionally with the improvement in  $J$ .

For nested loops, a simple prediction for  $\alpha$  can be made on the basis of distance shortening (Figures 2A and S2B). In the absence of the internal loop, the E-P tether is made up of the three DNA segments, abc (Figure 2A), giving  $J_{abc}$  for this loop. In the presence of the internal loop, a shorter E-P tether is formed by the a and c segments and the protein bridge, with  $J_{ac}$ . This gives  $\alpha = J_{ac}/J_{abc}$  (STAR Methods; Figure S3B). Discounting any effects of the protein bridge,  $J_{ac}$  should be similar to  $J$  for a single DNA segment with  $d = d_a + d_c$ . These  $J$  values can be estimated from the  $J$ -versus- $d$  relationship (Figure 1C). The expected  $\alpha$  values match the observed  $\alpha$  values reasonably well (Figure 2B). The  $\alpha$  values are high because  $J_{ac}$  for the 600 and 1,000 bp a + c distances is large relative to the low  $J_{abc}$  for the 20 kb E-P distance. The higher  $\alpha$  for the 300 + 300 bp a + c arrangement results from its larger  $J$  value, showing that loop assistance is stronger when the assisting sites are closer to the enhancer and promoter. This analysis shows that inside assisting loops can strongly stimulate NtrC enhancer action in a manner that is consistent with the increased relative concentration of the enhancer and promoter due to reduction of the effective E-P distance.

### Stimulation of Enhancer Action by Outside Loop Assistance

The distance-shortening effect should in theory apply equally well when the assisting looping elements are outside the E-P segment rather than inside (Figure 2C). Here the outside loop also provides a new E-P tether comprising the a and c DNA segments bridged by the looping protein (Figure 2C). The equation

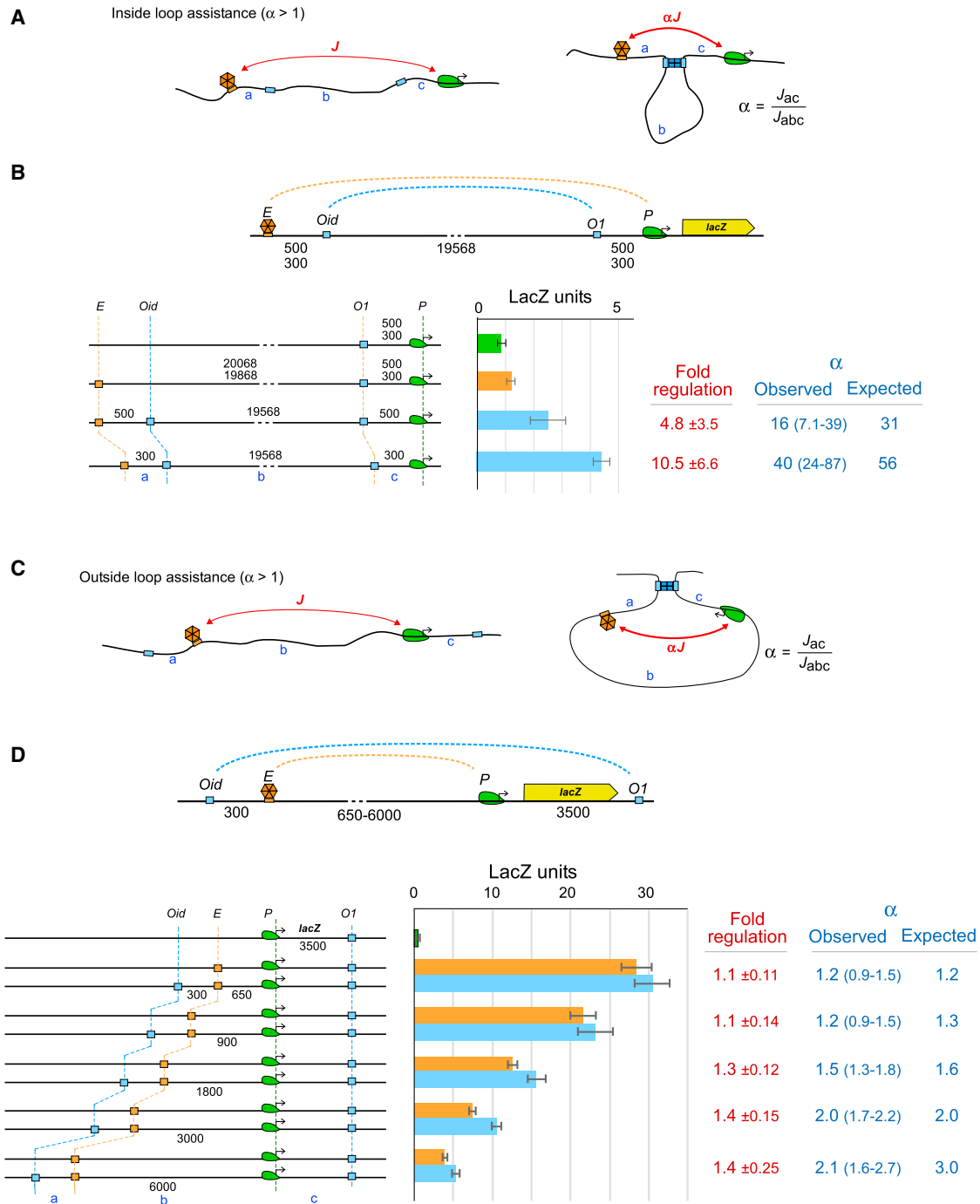


**Figure 2. Assisting Enhancer-Promoter Contact with Another DNA Loop**

(A) Loop assistance by an inside loop.  $\alpha$  is the change in  $J$  for the E-P interaction when the assisting loop is formed. For nested loops,  $\alpha$  is expected to be  $>1$ . (B) Promoter activity with  $\text{LacI}$  binding sites ( $O_{id}$  and  $O_1$ ) located 300 or 500 bp internally to the enhancer and promoter. Error bars are 95% confidence limits (Student's  $t$  test,  $n = 9$ ). Fold regulation is calculated as the ratio of the  $O_{id}^+O_1^+$  and  $O_{id}^-O_1^+$  units (the  $O_{id}^-O_1^+$  units were pooled) after subtraction of the  $E^-$  background. Errors are by error propagation. Medians (2.5th and 97.5th percentiles) of  $\alpha$  from 1,000 error-adjusted calculations are shown (STAR Methods). Expected  $\alpha$  values are calculated according to the equation in (A), using the  $J$ -versus- $d$  relationship (Figure 1C) and assuming that  $J_{ac}$  equals  $J$  for DNA of length  $a + c$ .

(C) Loop assistance by an outside loop.

(D) Assay of outside loop assistance. Calculations as in (B).

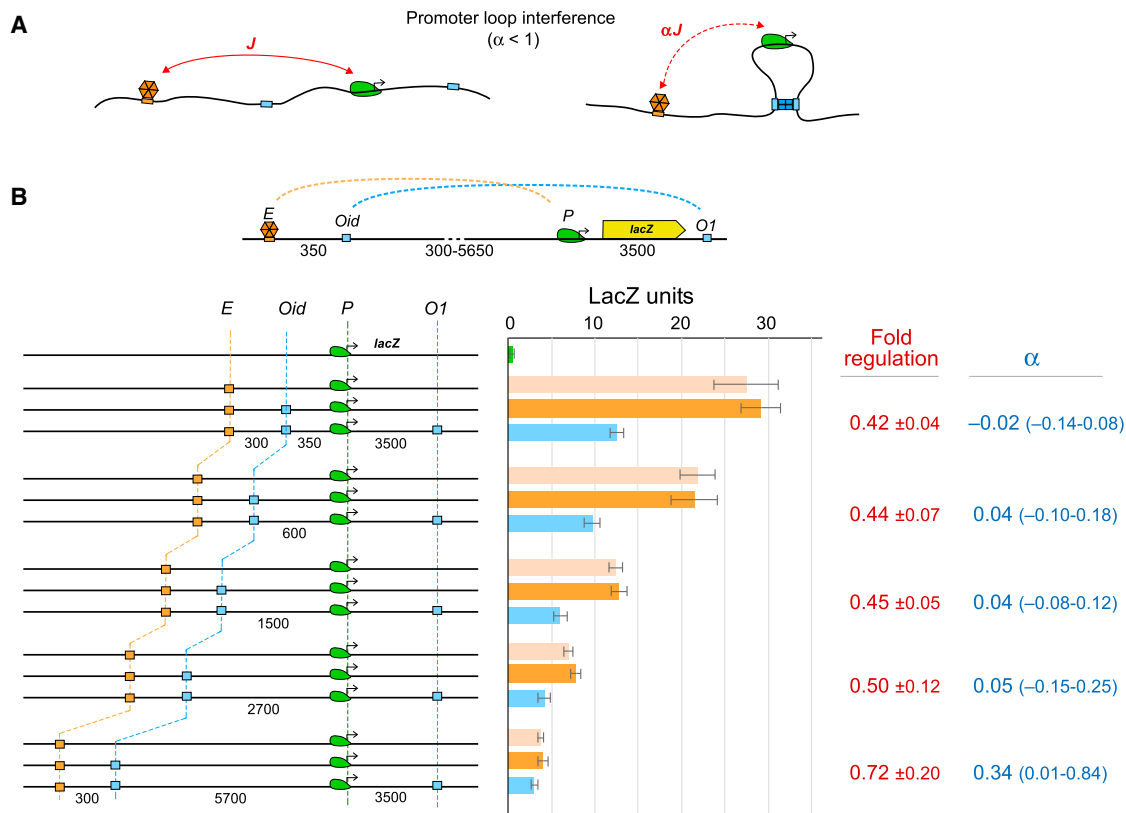


**Figure 3. Insulation by a Loop around the Promoter**

(A) Insulation causes a reduction in the effective relative concentration of the promoter and enhancer,  $J$ , by a factor  $\alpha$ , where  $\alpha < 1$ . The mechanism of insulation is not understood.

(B) Insulation effects for a *LacI* loop of different sizes around the promoter. Error bars are 95% confidence limits (Student's *t* test,  $n = 9-12$ ). Calculations and  $\alpha$  ranges as in Figure 2.

for  $\alpha$  is the same as for inside loop assistance (STAR Methods; Figure S2A).

To test outside loop assistance, we made reporters with a range of E-P spacings in which *Oid* was located 300 bp upstream of the enhancer and *O1* was located 3,500 bp downstream of the promoter (Figure 2D).

In the absence of the *LacI* loop, promoter activity fell with increasing E-P distance, as expected. In the presence of both *LacI* sites, although no significant loop assistance was seen when the direct E-P distance was short (650 or 900 bp), there was weak but significant loop assistance for the longer E-P spacings (1,800, 3,000, and 6,000 bp). Assistance is weak in this arrangement because the constant 3,800 bp  $a + c$  segment (300 + 3,500 bp) is long ( $J_{ac}$  is small), and only in the longer arrangements does  $J_{abc}$  become low enough to give a substantial increase in  $\alpha$ . Observed and expected  $\alpha$  values match well, indicating that stimulation of enhancer activity by outside loops is also consistent with the distance-shortening effect.

### A Loop around the Promoter Insulates It from the Enhancer

In the loop domain model of insulation, a DNA site within a loop is inhibited from interacting with DNA sites outside the loop. How-

ever, the mechanism of this inhibition is not clear. Quantitation of the magnitude of insulation and the factors that affect it should inform a better understanding. We have shown loop domain insulation using *LacI* and  $\lambda$  CI loops in *E. coli* cells (Priest et al., 2014a). Here, we report more extensive insulation experiments using the *NtrC* enhancer system.

We first examined insulation by a loop around the promoter (Figure 3A). We placed *Oid* between the promoter and the upstream enhancer and placed *O1* downstream of *lacZ* (Figure 3B). To examine geometry effects, we increased the length of the *LacI* loop, altering the E-P distance but keeping the distance between the enhancer and the *LacI* loop constant. In the absence of *O1*, promoter activity was as expected for each E-P distance and was unaffected by the presence of *Oid* in the E-P tether. However, in the presence of both *LacI* sites, clear insulation effects were apparent (Figure 3B).

$\alpha$  was estimated as for loop assistance (STAR Methods; Figure S3). In the case of insulation we expect  $\alpha < 1$ , that is, a reduction in  $J$  for E-P contact (Figure 3A), but the lack of a known mechanism for insulation means that it is not possible to obtain expected  $\alpha$  values. The observed  $\alpha$  values show strong insulation in most cases (Figure 3B). The negative  $\alpha$  value obtained for the 350 bp spacing is due to inhibition being greater than

expected even if the LacI loop completely inhibited E-P looping (STAR Methods; Figure S3C).

Changing the length of the LacI loop from 3,800 to 6,200 bp had little effect on  $\alpha$  values, indicating that insulation by a fully formed LacI loop around the promoter is reasonably insensitive to the size of the loop.

### A Loop around the Enhancer Insulates It from the Promoter

We next tested insulation by a loop around the enhancer (Figure 4A). We kept the length of the LacI loop constant at 600 bp (Figure 4B) and altered the E-P distance by moving the enhancer-containing LacI loop away from the promoter. We also varied the positioning of the LacI loop such that the enhancer was either centrally located or on the promoter-distal or promoter-proximal side (Figure 4B). We expected that insulation could be partially counteracted by an effective shortening of the E-P distance when the enhancer is in the distal location (Figure 4C).

LacI looping gave strong insulation, with an approximately 8-fold reduction of enhancer-dependent activity at the 650 bp E-P spacing, decreasing to an approximately 4-fold effect at the 6,000 bp spacing (Figure 4D, central constructs). The  $\alpha$  values also showed strong insulation by the LacI loop, ranging from about 30-fold at the 650 bp E-P spacing ( $\alpha = 0.03$ ) to about 4-fold at the 6,000 bp spacing ( $\alpha = 0.23$ ). Thus, there was a trend whereby the inhibitory effect of the LacI loop became weaker as the enhancer was moved further away from it.

These 600 bp enhancer insulating loops gave similar  $\alpha$  values to the 2,000 bp enhancer loops (Figure 4D, E-P 3,000 bp set), as well as the >3,800 bp promoter insulating loops (Figure 3B). This confirms that insulation is not strongly affected by the size of the insulating loop.

There was a weak but reasonably consistent effect of the distal, central, or proximal location of the enhancer within the LacI loop, with insulation weaker (higher  $\alpha$ ) for the distal location, consistent with the idea that distance shortening can partially counteract insulation (Figure 4C).

In conclusion, E-P contact in the NtrC-*glnAp2* system can be strongly inhibited by insulating loops placed either around the promoter or the enhancer.

### Two *glnAp2* Promoters Compete Weakly for the NtrC Enhancer

Having shown that the action of a bacterial enhancer is affected by DNA loops formed by another protein, we wished to test whether alternative DNA loops formed by the enhancer itself also affected activation.

Eukaryotic promoters sharing the same enhancer often compete with each other (Deng et al., 2014; Fukaya et al., 2016). The simplest explanation of competition is that it results from mutually exclusive contact with the enhancer, such that each promoter sequesters the enhancer from the other promoters. Mutually exclusive E-P contact seems likely for the NtrC-*glnAp2* system, as the compact active site of the NtrC complex and its close interaction with  $\sigma 54$  (Bush and Dixon, 2012; De Carlo et al., 2006) suggest that an NtrC enhancer can interact with only one closed complex at a time.

We tested whether two *glnAp2* promoters compete for activation by a shared NtrC enhancer by placing an enhancer downstream of *lacZ* controlled by a *glnAp2* promoter (P1) and varying the distance between the enhancer and an identical promoter (P2) located further downstream (Figure 5A). In control constructs, P2 was mutated to prevent RNAP binding (P2<sup>-</sup>; 4 of the 12 conserved positions altered). Competition at P1 should be stronger for shorter E-P2 distances because of stronger looping to P2. A very low level of competition at P1 was seen with an E-P2 spacing of 5,900 bp, increasing to about 27% competition at the 300 bp E-P2 spacing (Figure 5A). Thus, even when P2 was about 12-fold closer to the enhancer, the effect on P1 was moderate, showing weak promoter competition in this system.

We developed a thermodynamic model for competition in which the E-P2 interaction reduces the availability of the enhancer and thus,  $J_C$ , for the E-P1 interaction (Figure S4A). It is not known whether the NtrC enhancer also loops to the open complex, but we included it to maximize competition. Thus, looping to P2 is determined by the fraction of time P2 spends in the closed and open complexes,  $l$  for the interaction between the enhancer and these complexes (assumed equal), and  $J$  for the E-P2 tether. Because of reciprocal competition, looping to P2 is also dependent on the strength of the E-P1 interaction. Applying this model and fitting the five parameters ( $k_C$ ,  $k_U$ ,  $k_{O-max}$ ,  $k_e$ , and  $l_C$ ) to the competition data (STAR Methods; Figure S4A), we found that only E-P variants with  $l_C \leq \sim 5,000$  nM were able to produce a good fit (Figure 5B). Even allowing looping to the open complex, variants with  $l_C > 5,000$  nM produce too little competition because P2 loops too weakly to the enhancer to significantly reduce its availability for P1. Thus, the data provide an upper limit on  $l_C$  for our NtrC system and, combined with the limit imposed by the activity versus  $d$  data, constrain  $l_C$  to about 1,000–5,000 nM.

This range for  $l_C$  would give looping of 22%–59% at 300 bp and 1%–4% at 6,000 bp and is consistent with the 15%–20% looping seen *in vitro* for 370 and 460 bp E-P spacings in the homologous *Salmonella* NtrC-*glnAp2* system using electron and scanning force microscopy (Su et al., 1990; Rippe et al., 1997).

Importantly, E-P variants able to reproduce the competition and activity-versus-distance datasets were obtainable (Figure S4B). In some of these E-P variants, the closed  $\rightarrow$  open step is rate limiting, resulting in a high occupancy of the closed complex state (up to 78% at 300 bp), consistent with *in vitro* transcription assays (Friedman and Gelles, 2012; Ninfa et al., 1987) and *in vivo* footprinting (Sasse-Dwight and Gralla, 1988). For those variants giving at least 65% occupation of the closed complex state at 300 bp, the average time required for the free  $\rightarrow$  closed, closed  $\rightarrow$  open, and open  $\rightarrow$  elongating steps was 3.4, 10.4, and 1.6 s, respectively. These times are less than the  $\approx 10$ , 530, and 6 s seen for these steps in the single-molecule study of Friedman and Gelles (2012). However, as the overall firing rate *in vitro* was some 50-fold lower than ours, we suspect that sub-optimal *in vitro* conditions (e.g., use of relaxed DNA) are limiting the rates, particularly  $k_O$ .

### DNA Loop Control of E-P Specificity

We showed that assisting, insulating, and competing loops can be used individually to control E-P looping, but can these

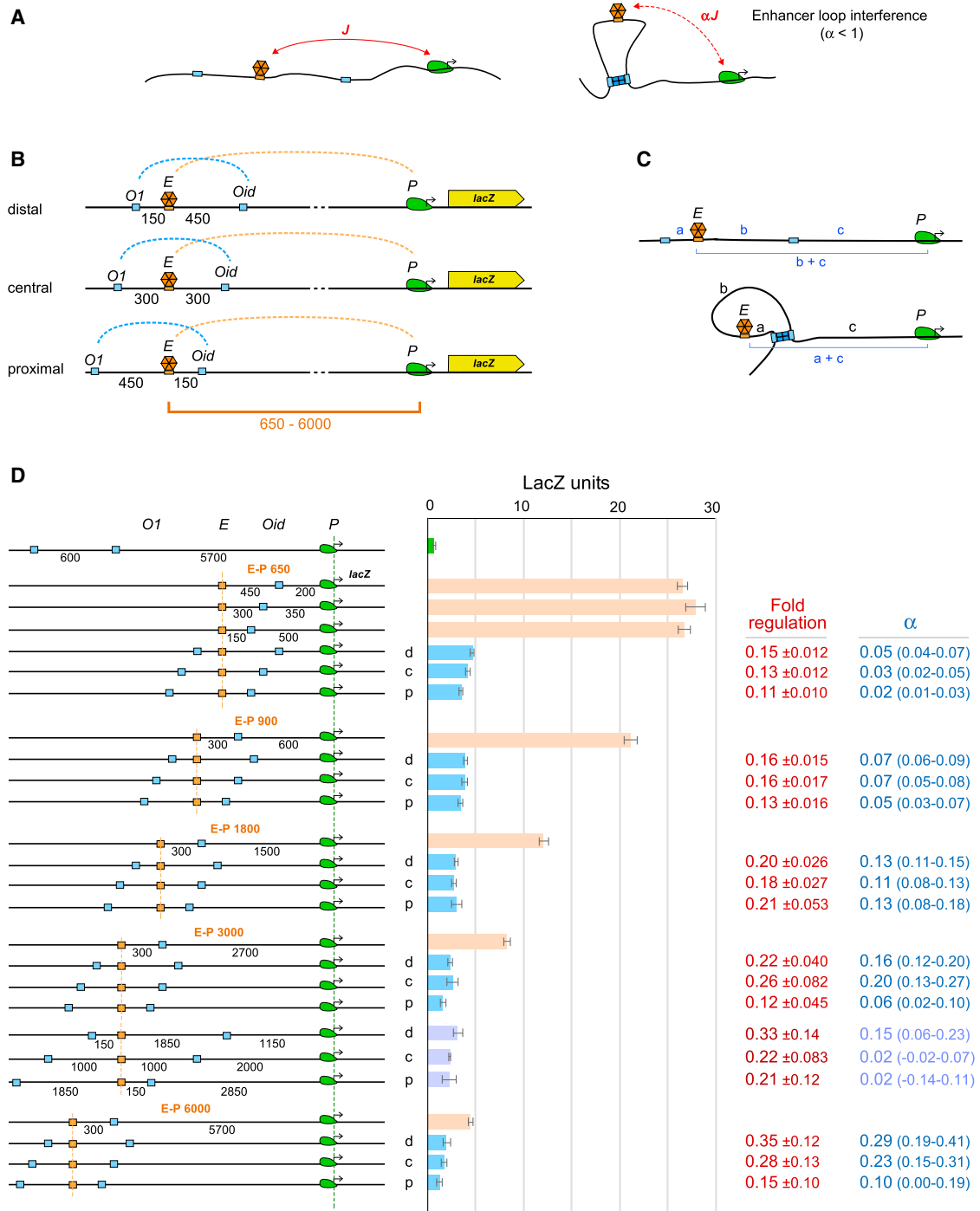


**Figure 4. Insulation by a Loop around the Enhancer**

(A) A loop around the enhancer is expected to reduce  $J$  for E-P contact.

(B) Constructs in which the location of the enhancer within the LacI loop is varied, while keeping the E-P distance fixed.

(C) A distal location of the enhancer causes LacI looping to shorten the effective E-P distance.

(D) Insulation effect of a LacI loop around the promoter over a range of E-P distances. Error bars are 95% confidence limits (Student's t test,  $n = 9$ ). Calculations and  $\alpha$  ranges as in Figure 2.

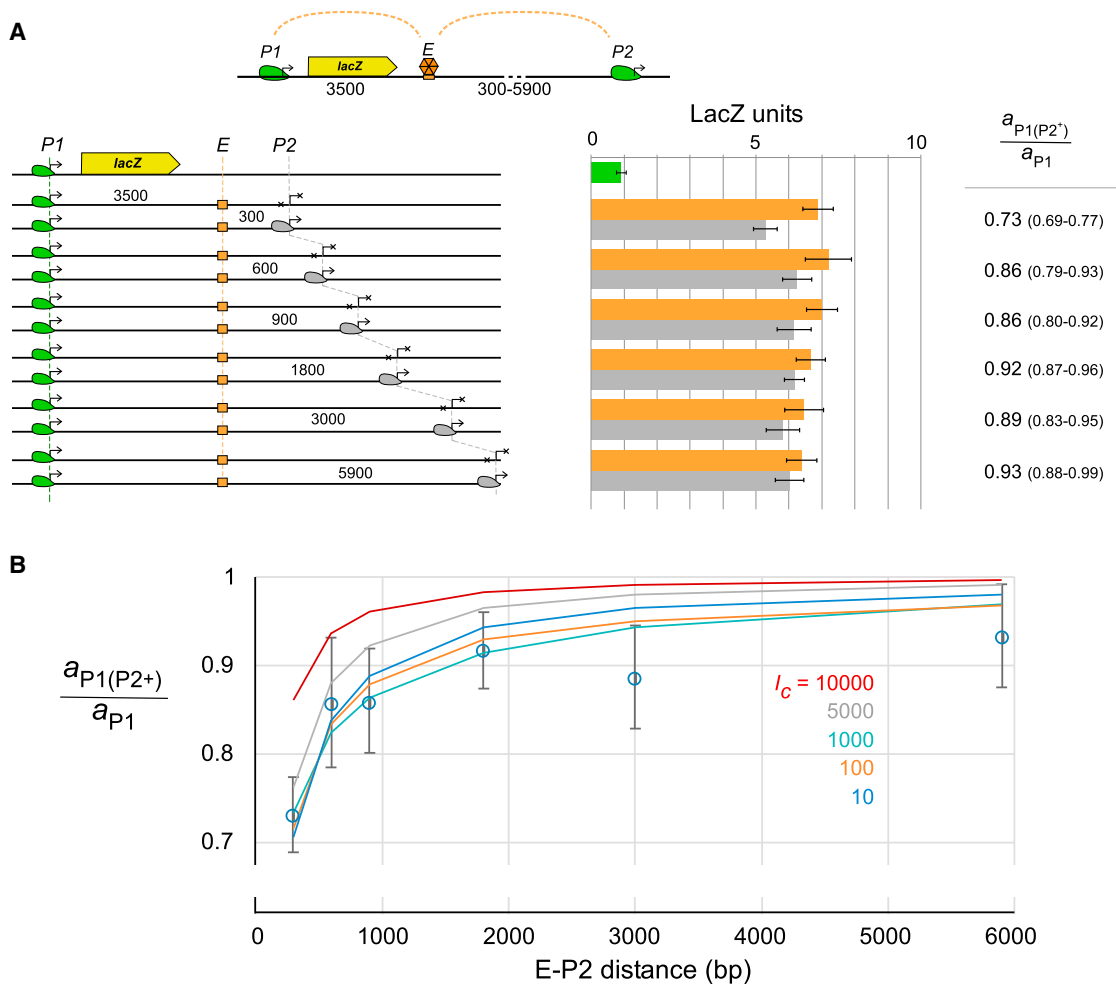


### Figure 5. Weak Competition between *glnAp2* Promoters for the Same Enhancer

(A) Effect of a second promoter (P2 or a P2<sup>-</sup> mutant), located at various distances from the enhancer, on enhancer activation of an identical promoter (P1) 3,600 bp away from the enhancer and expressing *lacZ*. The ratios of P1 activities ± P2 (E<sup>-</sup> backgrounds subtracted) are shown with 95% confidence intervals (Student's *t* test on logs of paired ratios, *n* = 15).

(B) Curves show optimal fits of the model to the competition data (A) obtained by adjusting  $k_C$ ,  $k_U$ ,  $k_{O-max}$ , and  $k_e$  (same values for both promoters) with different fixed  $I_C$  values (STAR Methods; Figure S4A). Note the truncated y axis.

mechanisms be combined to provide E-P specificity? To test this, we designed a dual-reporter construct (Figure 6A) in which the enhancer is downstream of the *lacZ* gene driven by one *glnAp2* promoter (P1) and is upstream of a tdTomato gene (*tom*) driven by a second *glnAp2* promoter (P2). Lac operators were located upstream of P1 and downstream of the enhancer such that LacI looping should give loop assistance for the E-P1 contact and simultaneously insulate the enhancer from P2. We also varied the E-P2 distance, while keeping the length of the LacI loop constant (Figure 6A).

In the absence of the LacI loop, P1 was active at a low level consistent with the 3,600 bp E-P1 distance. The activity of the E-P2.*tom* reporter varied with the E-P2 distance (Figure 6B), matching closely the *d* sensitivity seen with the *lacZ* reporter (Figure S5). In the presence of the LacI loop, P1 activity

increased about 5-fold, accompanied by an approximately 3-fold decrease in P2 activity at all E-P2 spacings (Figure 6B). The strong outside loop assistance for P1 is a result of the short 300 + 300 bp arms compared with the 3,600 bp E-P1 distance. The 3-fold insulation effect is consistent with that seen previously for a long LacI loop (Figure 3B). Thus, a single LacI loop was able to simultaneously confer loop assistance and loop interference to cause a 15-fold change in the relative activities of P1 and P2.

The effect of the LacI loop on competition between the promoters makes it difficult to calculate  $\alpha$  values in this experiment. The competition effect may explain why, in contrast to the results of Figure 4, we did not see a decrease in the insulating effect of the LacI loop on P2 as the E-P2 distance was increased.

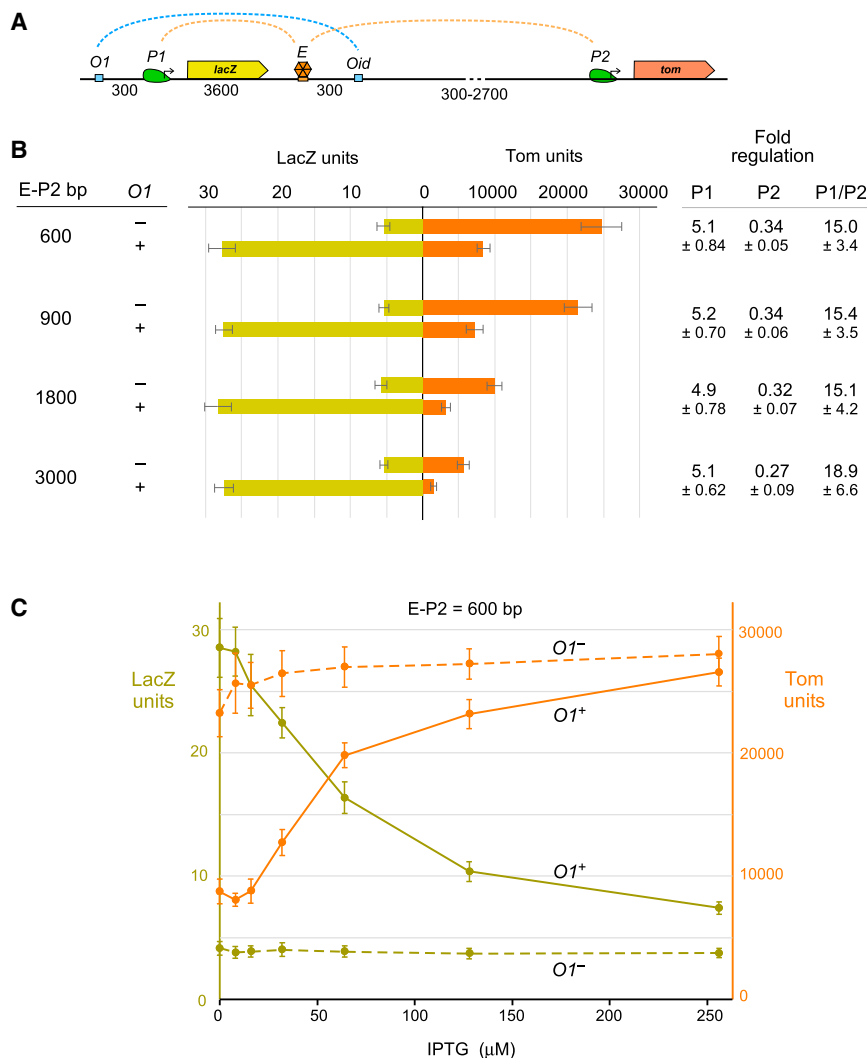


**Figure 6. Controlling Enhancer-Promoter Specificity**

(A) Schematic of the specificity reporter. P1 and P2 are identical *glnAp2* promoters controlled by a single NtrC enhancer.

(B) The presence ( $O1^+$ ) or absence ( $O1^-$ ) of the LacI loop shifts the relative enhancer-dependent activation of P1 and P2 by providing loop assistance for the E-P1 interaction and loop interference for the E-P2 interaction. Units have background values subtracted ( $E^-$  for LacZ, individual  $P2^-$  for Tom). Errors show 95% confidence limits (Student's t test,  $n = 9$ ).

(C) Inactivation of LacI looping by IPTG in the specificity reporter with the 600 bp E-P2 spacing progressively shifts enhancer activation from P1.lacZ to P2.tom. Units have background values subtracted ( $E^-$  for LacZ, individual  $P2^-$  for Tom). Errors show 95% confidence limits (Student's t test,  $n = 9$ ).

Control by other loops (loop assistance and insulation) or by alternative loops (promoter competition) has its effect by changing the availability of the enhancer and promoter for each other, that is, it modulates  $J_C$ . However, the way an E-P pair responds to changes in  $J_C$  is determined by E-P-specific parameters such as  $I_C$ , as well as the kinetic parameters.  $I_C$  determines how  $J_C$  affects the fraction of looping,  $F_C$ , and the kinetic parameters determine in turn how  $F_C$  affects activity (Figures 1C–1G). Different E-P variants thus have different  $J$  sensitivities, which can be seen in their different responses to E-P distance (Figure 1G).

Small ligand stimulation of E-P contact was demonstrated by Morgan et al. (2017), who showed that an S-(+)-abscisic acid could be used to activate human  $\beta$ -globin expression by inducing dimerization of a pair of dCas9-fusion proteins, assisting E-P looping. We used inhibition of LacI DNA binding by IPTG to modulate E-P specificity in the NtrC system. IPTG was able to produce a progressive, concentration-dependent shift in enhancer activity from P1 favoring to P2 favoring, showing small molecule control of E-P specificity (Figure 6C).

### E-P Properties Determine the Responsiveness to DNA Looping Control

Our results show that the NtrC-*glnAp2* system is sensitive to control by loops formed by another protein but is not highly sensitive to competition by another promoter. Are these general properties of E-P systems or could different E-P pairs respond differently to loop control? Our model of enhancer action and loop interactions allowed us to explore this question.

We simulated E-P distance, loop assistance, insulation, and promoter competition scenarios for a selection of E-P variants having a range of  $I_C$  values (10, 100, 1,000, or 10,000 nM). This large range of  $I_C$  values is feasible; we have estimated  $I$  values of about 5 nM for the interaction between two sets of four  $\lambda$  CI binding sites, about 35–80 nM for pairs of Lac operators (Hao et al., 2017a) and now 1,000–5,000 nM for NtrC-*glnAp2*. Within each  $I_C$  class, kinetic variants were chosen that maximized or minimized  $J$  sensitivity (parameters listed in Figure S6A).

This range of  $J$  sensitivity produces large differences in sensitivity to E-P distance. For the most  $J$ -sensitive E-P variant, activity drops 5-fold as  $d$  is increased from 300 to 1,500 bp ( $I_C = 10,000$  nM; Figure 7A, red line). For the least  $J$ -sensitive variant,  $d$  must be increased to about 1 Mbp to decrease activity 5-fold ( $I_C = 10$  nM; Figure 7A, blue line).

To simulate loop assistance, the scenario was a 6,000 bp E-P distance with assisting looping elements nested 400 bp internally (Figure 7B), giving an expected  $\alpha$  of 10.2. The plots show the changes in activity as the controlling loop

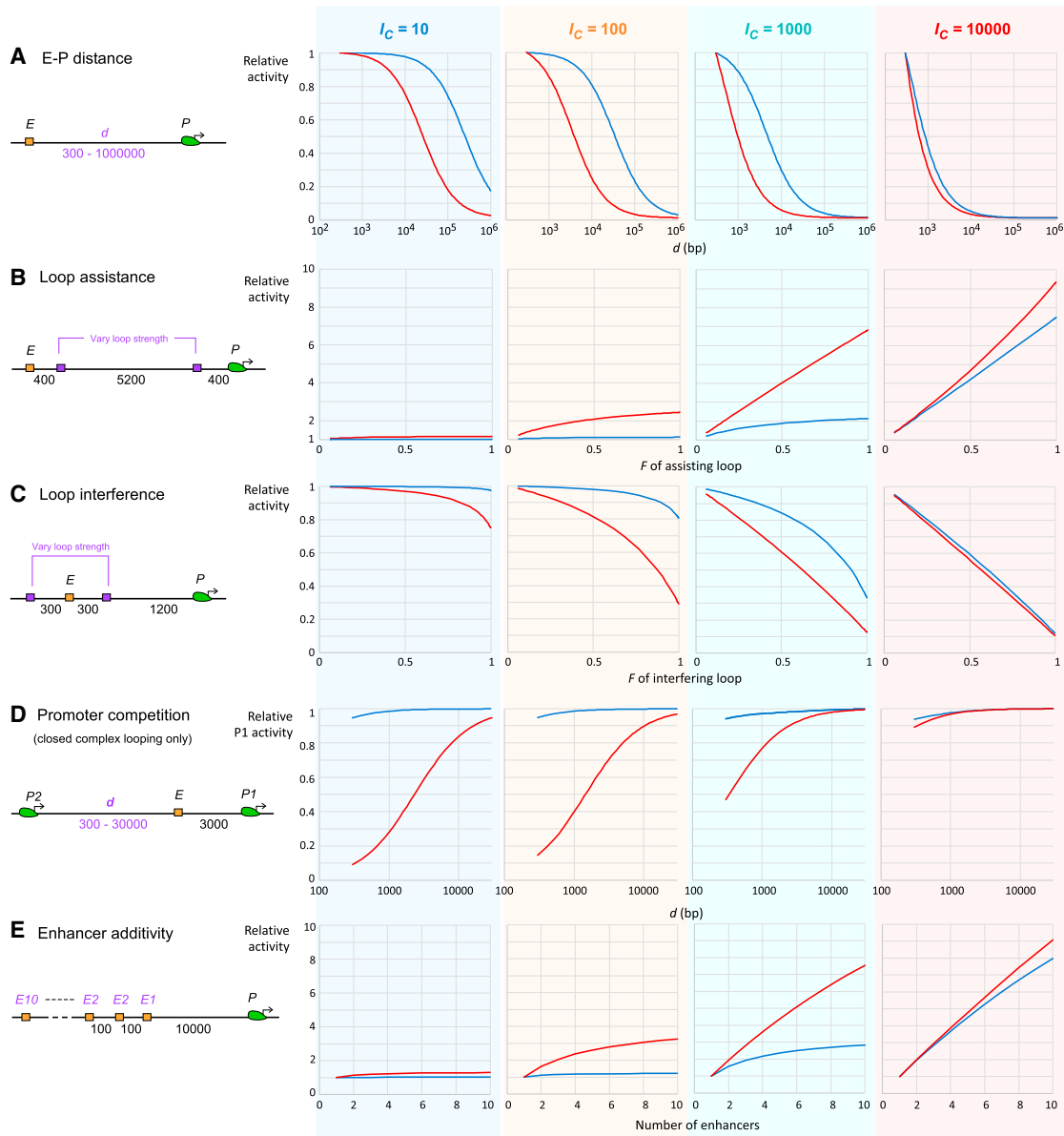


**Figure 7. Tunability of the E-P Response to DNA Looping**

(A) Distance sensitivity of eight E-P variants with different  $I_C$  values (10, 100, 1,000, or 10,000 nM) and kinetic parameters. The red curves are variants where the closed  $\rightarrow$  open reaction is maximally rate limiting ( $k_o$  limited, closed complex dominated). The blue curves are variants where the closed  $\rightarrow$  open reaction is minimally rate limiting ( $k_c/k_e$  limited, closed complex rare). Parameters are listed in Figure S6A.

(B) Expected loop assistance for the E-P variants for a configuration with an expected  $\alpha$  of 10.2. Plots show the fold change in activity as the strength of the assisting loop is increased, as measured by its calculated fractional looping  $F$  in the absence of E and P.

(C) Expected insulation for the E-P variants for  $\alpha = 0.1$ .

(D) Expected relative activity of P1 in the presence of an identical promoter (P2). The E-P1 distance was fixed at 3,000 bp and the E-P2 distance was varied.

(E) Expected relative promoter activity in the presence of identical multiple enhancers.

is strengthened. The E-P variants' responses to loop assistance ranged from almost completely insensitive to highly sensitive, with loop sensitivity correlating with  $J$  sensitivity (Figure 7B).

To simulate insulation, the scenario was a 1,500 bp E-P distance with a 600 bp interfering loop around the enhancer (Figure 7C), assigned  $\alpha = 0.1$  (see Figure 3B). Again, there were large

differences in responsiveness to insulation, with sensitivity again correlating with  $J$  sensitivity (Figure 7C).

Thus, sensitivity of enhancer action to positive or negative control by other DNA loops is strongly dependent on the parameters of the E-P pair.

To simulate competition between identical promoters, the scenario was an E-P1 distance of 3,000 bp, with the second

promoter (P2) at 300–30,000 bp from the enhancer (Figure 7D). Here we allowed looping only to the closed complex, but similar results were obtained if open complex looping was allowed (Figure S6B). Competition was under strong kinetic control, with the more  $J$ -insensitive variants within each  $I_C$  class showing little competition regardless of  $I_C$  (Figure 7D). In these variants, where the closed  $\rightarrow$  open reaction is fast, the closed complex is rare and there is little looping to P1 or P2. However, lower  $I_C$  values allow a large scope for competition if the kinetics favor closed complex formation, because of stronger looping. Thus, sensitivity to promoter competition is also strongly affected by enhancer-promoter parameters, though in a different way from control by other loops.

We also simulated alternative loop control in which a single promoter is activated by multiple enhancers (Figure 7E). Additional enhancers effectively increase  $J_C$  for E-P interactions. Accordingly, we found that increasing the number of enhancers gave similar results to loop assistance (Figure 7B), with  $J$ -sensitive E-P pairs displaying almost linear increases in activity with increasing numbers of enhancers (enhancer additivity) and  $J$ -insensitive E-P pairs increasing very little (enhancer subadditivity).

## DISCUSSION

Our results demonstrating E-P targeting (loop assistance), insulation, and promoter competition in the NtrC-*glnAp2* system extend the similarities between bacterial and eukaryotic enhancers and further validate these simple systems as models for analysis of enhancer function. Importantly, we showed that these mechanisms could be combined to give a 15-fold change in E-P specificity. Thus, the NtrC system should enable testing of specificity control by more complex combinations of loops.

We showed that the three mechanisms of loop control can be rationalized as changing the effective relative concentration of the enhancer and promoter, that is, as altering  $J$ . What do our results tell us about the mechanisms of this “ $J$  manipulation”?

### Loop Assistance

E-P activity was assisted when LacI formed a DNA loop either inside or outside the E-P loop. The magnitude of assistance quantified by the parameter  $\alpha$  was generally consistent with the increase in  $J_C$  expected if the two DNA arms bridged by LacI provided a shorter E-P tether between E and P. That is, loop assistance acts by a distance shortening mechanism. These findings are consistent with our previous measurements with LacI and  $\lambda$ CI loops (Hao et al., 2017a; Priest et al., 2014a), as well as chromatin modeling (Doyle et al., 2014). As expected from this mechanism, assistance was stronger when the distance between the assisting sites and the enhancer and promoter was shorter and when the initial E-P distance was longer. Thus, we expect that dedicated targeting elements will be most effective when located near the enhancer and promoter and when E-P looping is initially weak. However, significant loop assistance should also occur when the looping elements are distant from the promoter and enhancer. The pervasive looping in eukaryotic genomes means that, at least some of the time, enhancers and promoters are linked by protein-bridged tethers

that are much shorter than the distance between them along the DNA.

### Insulation

E-P activity was inhibited when LacI formed a loop that contained the enhancer or the promoter but not both, consistent with the loop domain model for insulation. Insulation was strong, with  $\alpha$  varying over the range of about 0.3–0.03 (Figures 3 and 4). It is difficult to compare this with eukaryotic insulation, because estimates of absolute loop interactions are not available. However, the regulatory effect of LacI loop insulation on NtrC enhancer activity was about 2-fold to 9-fold (Figures 3B and 4C), comparable with eukaryotic insulation effects; a 3-fold decrease in RNAP chromatin immunoprecipitation signal was seen upon insertion of a CTCF insulator at the human  $\beta$ -globin locus (Hou et al., 2008), and a 5-fold inhibition of transcription was caused by insertion of a *gypsy* insulator in *Drosophila* (Fukaya et al., 2016).

The mechanism of insulation remains a puzzle. However, our measurements provide some constraints for possible models. As well as providing up to 30-fold insulation, models should be able to reproduce loop size independence, where similar insulation occurs with loops ranging from 600 to 3,800 bp, and also decreasing insulation with increasing E-P distance.

Single-molecule experiments (Priest et al., 2014a) and chromatin modeling (Doyle et al., 2014) with naked, relaxed DNA suggest that some insulation results from the DNA of the loop shielding the internal site. This mechanism is akin to the proposed “eclipse” effect of an obstructing protein bound near the enhancer or the promoter (Pollak et al., 2017). However, only about 2-fold insulation was seen (Doyle et al., 2014; Priest et al., 2014a), substantially less than we saw *in vivo*. In addition, the modeled insulation did not reproduce sensitivity to the E-P distance.

It is likely that insulation is dependent on the packaging of DNA *in vivo*. DNA inside cells is thought to be packaged into relatively unknotted “blobs,” for example, as in the fractal globule model (Lieberman-Aiden et al., 2009). Although the  $-1.1$  decay exponent for the  $J$ -versus-distance power law in *E. coli* (Priest et al., 2014b; Figure S2A) is consistent with this model, it is not clear to us what predictions this model makes for insulation by DNA loops.

Our preferred model for insulation is that the insulating loop acts by removing the stimulation of interaction caused by DNA supercoiling. Supercoiling causes intertwining and compaction of DNA within the same loop or domain. This effect strongly aids interactions between sites within the same supercoiled domain in simulations (Benedetti et al., 2014) and in single-molecule experiments (Yan et al., 2018). Indeed, long-range NtrC activation of the *glnAp2* promoter on plasmids *in vitro* was stimulated up to 50-fold by DNA supercoiling (Liu et al., 2001). Importantly, this supercoiling stimulation of activation was strongly inhibited by a LacI loop that placed the enhancer and promoter into separate domains, showing insulation *in vitro* (Bondarenko et al., 2003). A supercoil domain model is thus consistent with strong insulation *in vivo*, as well as loop size independence, because domain separation results from insulating loops of any size. *E. coli* DNA is thought to be organized into random negatively supercoiled loops averaging about 10 kb (Postow et al., 2004), with loops possibly anchored

by non-specific DNA-binding proteins (e.g., MukB) (Kumar et al., 2017). Our reduced insulation with increasing E-P distance might thus be explained as due to an increasing likelihood that the enhancer and promoter are already in separate loops, in which case adding the LacI loop would have no effect. The close to linear decay of contact probability with DNA distance may also reflect in part this increased chance of the interacting sites being in separate loops. A role for negative supercoiling in eukaryotic E-P communication is not clear (Gilbert and Allan, 2014), but modeling suggests that transcription-induced supercoiling in eukaryotes could aid E-P interactions (Benedetti et al., 2017).

### Promoter Competition

Our promoter competition results are consistent with mutually exclusive E-P contact, where looping of the enhancer to one promoter sequesters it from interaction with the other promoter, as proposed to explain promoter competition in eukaryotes. However, mutually exclusive E-P contact has been challenged by recent live cell imaging studies in *Drosophila* showing apparent simultaneous activation of two promoters by a single enhancer (Fukaya et al., 2016; Lim et al., 2018). It is proposed that the enhancer and promoters form a three-way interaction within a pool of RNA polymerase II and transcription activators that are able to be used simultaneously by both promoters (Lim et al., 2018). However, it is hard to reconcile this model with the competitive effects seen between the two promoters, because it implies that activity of one promoter must deplete the shared resources, resulting in simultaneous non-activity of the other promoter. It is possible that the apparent co-activation may result from rapid alternate pairwise contacts, as suggested by Bartman et al. (2016) for dual promoter activation at the  $\beta$ -globin locus.

### E-P Parameters Determine the Response to Control by Other DNA Loops

A striking result of our modeling is that the response of an E-P pair to  $J$  manipulation is strongly dependent on thermodynamic and kinetic parameters that determine  $J$  sensitivity (Figure 7). For  $J$ -sensitive E-P pairs, such as the NtrC-*glnAp2* case, activation is sensitive to distance and to assisting or insulating DNA loops. Competitive effects between such E-P pairs are weak, allowing one enhancer to effectively activate multiple promoters and multiple enhancers to work additively at a single promoter. At the  $J$ -insensitive extreme, E-P pairs are active over very large distances and are relatively resistant to assistance or insulation. Such E-P pairs should display strong competition between promoters, and subadditivity, even redundancy, of multiple enhancers.

The primary parameter determining  $J$  sensitivity is the strength of interaction between the enhancer and promoter, represented by  $l$ . For a specific E-P arrangement (a fixed  $J$ ),  $l$  determines the fraction of time  $F$  that the enhancer and promoter spend in contact. Lower  $l$  values give strong looping that is less  $J$  sensitive; higher  $l$  values give weak looping that is more  $J$  sensitive. Kinetic parameters have a secondary impact on  $J$  sensitivity, determining how  $F$  affects activation. If the looping-dependent reactions are slow relative to the other reactions, then  $J$  sensitivity is maximized; if the looping-dependent reactions are fast relative to the other reactions, then  $J$  sensitivity is minimized. Although

promoter activation by eukaryotic enhancers is more complex than our simple E-P model, involving many kinetic steps and possibly multiple steps that are looping dependent, these principles should still apply.

We expect that these parameters could be tuned by evolution to create large differences in  $J$  sensitivity between different E-P pairs, causing different eukaryotic E-P pairs to vary in their responses to assisting, insulating, and competing loops. We have estimated  $l$  values of about 35 nM for pairs of Lac operators and about 5 nM for the interaction between two sets of four  $\lambda$  CI binding sites (Hao et al., 2017a). Equivalent or stronger E-P interactions should be achievable by the large protein complexes that assemble at eukaryotic enhancers and promoters. Chen et al. (2018) reported an 8% frequency of microscopic colocalization in live nuclei of sequences near two *homie* insulators separated by 142 kb, with no colocalization if one *homie* was removed. An interaction of this frequency in *E. coli* DNA could be achieved with  $l = 14$  nM, which would place *homie* interactions in the  $J$  insensitive class. Weaker E-P interactions, such as  $l = 1,000$ – $5,000$  nM for the NtrC-*glnAp2* system, must also be accessible for eukaryotic E-P pairs. Although *in vivo* rates of looping-dependent and looping-independent kinetic reactions for eukaryotic E-P pairs are unknown, we imagine that differences in these rates could also contribute strongly to differences in  $J$  sensitivity.

Some differences in the  $J$  sensitivity of different E-P pairs can be inferred from observed differences in enhancer additivity. Bothma et al. (2015) placed different enhancers at two locations upstream of a promoter and found that the weaker enhancers gave additive activation, while the stronger enhancers gave subadditive activation. This result implies that the subadditive enhancers are less  $J$  sensitive (Figure 7E). The model of Bothma et al. (2015) assumes that the stronger enhancers loop more strongly to the promoter and thus tend to sequester the promoter from each other. Although this lower  $l$  explanation is consistent with our model, the difference in additivity could also arise from differences in kinetics, for example, if the looping-dependent reactions were faster for the stronger E-P pairs. In this case, subadditivity of two strong enhancers is because some other kinetic step at the promoter becomes limiting.

We expect that  $J$  sensitivity will vary not just between different E-P pairs but also for a single E-P pair in a condition-dependent way. Changes in the composition or modification states of the protein complexes bound at the enhancer or promoter are likely to affect E-P interaction strength and kinetic parameters. Indeed, enhancer additivity can change with cell type and development (Bothma et al., 2015; Lam et al., 2015). Thus, the way an E-P pair responds to the effects of other DNA loops or to the presence of other promoters or enhancers should be regulatable by developmental and environmental signals.

### STAR★METHODS

Detailed methods are provided in the online version of this paper and include the following:

- KEY RESOURCES TABLE
- CONTACT FOR REAGENT AND RESOURCE SHARING

- EXPERIMENTAL MODEL AND SUBJECT DETAILS
  - Strain constructions
- METHOD DETAILS
  - Reporter assays
  - Modeling enhancer activation
  - Modeling effects of other DNA loops
- QUANTIFICATION AND STATISTICAL ANALYSIS

## SUPPLEMENTAL INFORMATION

Supplemental Information can be found with this article online at <https://doi.org/10.1016/j.celrep.2019.02.002>.

## ACKNOWLEDGMENTS

We thank Kim Sneppen for careful reading of the manuscript and Bomyi Li and members of the Shearwin lab for discussions. The work was funded by NHMRC grant GNT1100651, an ARC Discovery Early Career Researcher Award to N.H. (DE150100091), and an ARC Discovery grant (DP160101450). N.H. was also funded in part through the CSIRO Synthetic Biology Future Science Platform.

## AUTHOR CONTRIBUTIONS

Conceptualization, N.H., K.E.S., and I.B.D.; Methodology, N.H., K.E.S., and I.B.D.; Investigation, N.H.; Formal Analysis, I.B.D.; Writing – Original Draft, I.B.D.; Writing – Review & Editing, N.H., K.E.S., and I.B.D.; Resources, N.H., K.E.S., and I.B.D.; Funding Acquisition, N.H., K.E.S., and I.B.D.

## DECLARATIONS OF INTEREST

The authors declare no competing interests.

Received: November 7, 2018

Revised: January 8, 2019

Accepted: February 1, 2019

Published: February 26, 2019

## REFERENCES

Amit, R., Garcia, H.G., Phillips, R., and Fraser, S.E. (2011). Building enhancers from the ground up: a synthetic biology approach. *Cell* **146**, 105–118.

Bartman, C.R., Hsu, S.C., Hsiung, C.C.S., Raj, A., and Blobel, G.A. (2016). Enhancer regulation of transcriptional bursting parameters revealed by forced chromatin looping. *Mol. Cell* **62**, 237–247.

Benedetti, F., Dorier, J., and Stasiak, A. (2014). Effects of supercoiling on enhancer-promoter contacts. *Nucleic Acids Res.* **42**, 10425–10432.

Benedetti, F., Racko, D., Dorier, J., Burnier, Y., and Stasiak, A. (2017). Transcription-induced supercoiling explains formation of self-interacting chromatin domains in *S. pombe*. *Nucleic Acids Res.* **45**, 9850–9859.

Bondarenko, V.A., Jiang, Y.I., and Studitsky, V.M. (2003). Rationally designed insulator-like elements can block enhancer action in vitro. *EMBO J.* **22**, 4728–4737.

Bothma, J.P., Garcia, H.G., Ng, S., Perry, M.W., Gregor, T., and Levine, M. (2015). Enhancer additivity and non-additivity are determined by enhancer strength in the *Drosophila* embryo. *eLife* **4**, 1–14.

Bush, M., and Dixon, R. (2012). The role of bacterial enhancer binding proteins as specialized activators of  $\sigma 54$ -dependent transcription. *Microbiol. Mol. Biol. Rev.* **76**, 497–529.

Chen, H., Levo, M., Barinov, L., Fujioka, M., Jaynes, J.B., and Gregor, T. (2018). Dynamic interplay between enhancer-promoter topology and gene activity. *Nat. Genet.* **50**, 1296–1303.

Chetverina, D., Aoki, T., Erokhin, M., Georgiev, P., and Schedl, P. (2014). Making connections: insulators organize eukaryotic chromosomes into independent cis-regulatory networks. *BioEssays* **36**, 163–172.

Cho, S.W., Xu, J., Sun, R., Mumbach, M.R., Carter, A.C., Chen, Y.G., Yost, K.E., Kim, J., He, J., Nevins, S.A., et al. (2018). Promoter of lncRNA gene PVT1 is a tumor-suppressor DNA boundary element. *Cell* **173**, 1398–1412.e22.

De Carlo, S., Chen, B., Hoover, T.R., Kondrashkina, E., Nogales, E., and Nixon, B.T. (2006). The structural basis for regulated assembly and function of the transcriptional activator NtrC. *Genes Dev.* **20**, 1485–1495.

Deng, W., Rupon, J.W., Krivega, I., Breda, L., Motta, I., Jahn, K.S., Reik, A., Gregory, P.D., Rivella, S., Dean, A., and Blobel, G.A. (2014). Reactivation of developmentally silenced globin genes by forced chromatin looping. *Cell* **158**, 849–860.

Dixon, J.R., Selvaraj, S., Yue, F., Kim, A., Li, Y., Shen, Y., Hu, M., Liu, J.S., and Ren, B. (2012). Topological domains in mammalian genomes identified by analysis of chromatin interactions. *Nature* **485**, 376–380.

Doyle, B., Fudenberg, G., Imakaev, M., and Mirny, L.A. (2014). Chromatin loops as allosteric modulators of enhancer-promoter interactions. *PLoS Comput. Biol.* **10**, e1003867.

Dunaway, M., and Dröge, P. (1989). Transactivation of the *Xenopus* rRNA gene promoter by its enhancer. *Nature* **341**, 657–659.

Dunham, I., Kundaje, A., Aldred, S.F., Collins, P.J., Davis, C.A., Doyle, F., Epstein, C.B., Frieze, S., Harrow, J., Kaul, R., et al.; ENCODE Project Consortium (2012). An integrated encyclopedia of DNA elements in the human genome. *Nature* **489**, 57–74.

Friedman, L.J., and Gelles, J. (2012). Mechanism of transcription initiation at an activator-dependent promoter defined by single-molecule observation. *Cell* **148**, 679–689.

Fukaya, T., Lim, B., and Levine, M. (2016). Enhancer control of transcriptional bursting. *Cell* **166**, 358–368.

Furlong, E.E.M., and Levine, M. (2018). Developmental enhancers and chromosome topology. *Science* **361**, 1341–1345.

Gilbert, N., and Allan, J. (2014). Supercoiling in DNA and chromatin. *Curr. Opin. Genet. Dev.* **25**, 15–21.

Hao, N., Krishna, S., Ahlgren-Berg, A., Cutts, E.E., Shearwin, K.E., and Dodd, I.B. (2014). Road rules for traffic on DNA-systematic analysis of transcriptional roadblocking in vivo. *Nucleic Acids Res.* **42**, 8861–8872.

Hao, N., Sneppen, K., Shearwin, K.E., and Dodd, I.B. (2017a). Efficient chromosomal-scale DNA looping in *Escherichia coli* using multiple DNA-looping elements. *Nucleic Acids Res.* **45**, 5074–5085.

Hao, N., Shearwin, K.E., and Dodd, I.B. (2017b). Programmable DNA looping using engineered bivalent dCas9 complexes. *Nat. Commun.* **8**, 1628.

Hou, C., Zhao, H., Tanimoto, K., and Dean, A. (2008). CTCF-dependent enhancer-blocking by alternative chromatin loop formation. *Proc. Natl. Acad. Sci. U S A* **105**, 20398–20403.

Kieffer-Kwon, K.R., Tang, Z., Mathe, E., Qian, J., Sung, M.H., Li, G., Resch, W., Baek, S., Pruetz, N., Grøntved, L., et al. (2013). Interactome maps of mouse gene regulatory domains reveal basic principles of transcriptional regulation. *Cell* **155**, 1507–1520.

Kumar, R., Grosbart, M., Nurse, P., Bahng, S., Wyman, C.L., and Marians, K.J. (2017). The bacterial condensin MukB compacts DNA by sequestering supercoils and stabilizing topologically isolated loops. *J. Biol. Chem.* **292**, 16904–16920.

Kvon, E.Z., Kazmar, T., Stampfel, G., Yáñez-Cuna, J.O., Pagani, M., Scherhuber, K., Dickson, B.J., and Stark, A. (2014). Genome-scale functional characterization of *Drosophila* developmental enhancers in vivo. *Nature* **512**, 91–95.

Lam, D.D., de Souza, F.S.J., Nasif, S., Yamashita, M., López-Leal, R., Otero-Corchon, V., Meece, K., Sampath, H., Mercer, A.J., Wardlaw, S.L., et al. (2015). Partially redundant enhancers cooperatively maintain mammalian gene expression above a critical functional threshold. *PLoS Genet.* **11**, e1004935.

- Liang, S., Bipatnath, M., Xu, Y., Chen, S., Dennis, P., Ehrenberg, M., and Bremer, H. (1999). Activities of constitutive promoters in *Escherichia coli*. *J. Mol. Biol.* 292, 19–37.
- Lieberman-Aiden, E., van Berkum, N.L., Williams, L., Imakaev, M., Ragozcy, T., Telling, A., Amit, I., Lajoie, B.R., Sabo, P.J., Dorschner, M.O., et al. (2009). Comprehensive mapping of long-range interactions reveals folding principles of the human genome. *Science* 326, 289–293.
- Lim, B., Heist, T., Levine, M., and Fukaya, T. (2018). Visualization of transvection in living *Drosophila* embryos. *Mol. Cell* 70, 287–296.e6.
- Liu, Y., Bondarenko, V., Ninfa, A., and Studitsky, V.M. (2001). DNA supercoiling allows enhancer action over a large distance. *Proc. Natl. Acad. Sci. USA* 98, 14883–14888.
- Long, H.K., Prescott, S.L., and Wsocka, J. (2016). Ever-changing landscapes: transcriptional enhancers in development and evolution. *Cell* 167, 1170–1187.
- Morgan, S.L., Mariano, N.C., Bermudez, A., Arruda, N.L., Wu, F., Luo, Y., Shankar, G., Jia, L., Chen, H., Hu, J.F., et al. (2017). Manipulation of nuclear architecture through CRISPR-mediated chromosomal looping. *Nat. Commun.* 8, 15993.
- Mumbach, M.R., Satpathy, A.T., Boyle, E.A., Dai, C., Gowen, B.G., Cho, S.W., Nguyen, M.L., Rubin, A.J., Granja, J.M., Kazane, K.R., et al. (2017). Enhancer connectome in primary human cells identifies target genes of disease-associated DNA elements. *Nat. Genet.* 49, 1602–1612.
- Ninfa, A.J., Reitzer, L.J., and Magasanik, B. (1987). Initiation of transcription at the bacterial *glnAp2* promoter by purified *E. coli* components is facilitated by enhancers. *Cell* 50, 1039–1046.
- Pioszak, A.A., and Ninfa, A.J. (2003). Genetic and biochemical analysis of phosphatase activity of *Escherichia coli* NRII (NtrB) and its regulation by the PII signal transduction protein. *J. Bacteriol.* 185, 1299–1315.
- Pollak, Y., Goldberg, S., and Amit, R. (2017). A looping-based model for quenching repression. *PLoS Comput. Biol.* 13, e1005337.
- Postow, L., Hardy, C.D., Arsuaga, J., and Cozzarelli, N.R. (2004). Topological domain structure of the *Escherichia coli* chromosome. *Genes Dev.* 18, 1766–1779.
- Priest, D.G., Kumar, S., Yan, Y., Dunlap, D.D., Dodd, I.B., and Shearwin, K.E. (2014a). Quantitation of interactions between two DNA loops demonstrates loop domain insulation in *E. coli* cells. *Proc. Natl. Acad. Sci. U S A* 111, E4449–E4457.
- Priest, D.G., Cui, L., Kumar, S., Dunlap, D.D., Dodd, I.B., and Shearwin, K.E. (2014b). Quantitation of the DNA tethering effect in long-range DNA looping in vivo and in vitro using the Lac and  $\lambda$  repressors. *Proc. Natl. Acad. Sci. U S A* 111, 349–354.
- Rao, S.S.P., Huntley, M.H., Durand, N.C., Stamenova, E.K., Bochkov, I.D., Robinson, J.T., Sanborn, A.L., Machol, I., Omer, A.D., Lander, E.S., and Aiden, E.L. (2014). A 3D map of the human genome at kilobase resolution reveals principles of chromatin looping. *Cell* 159, 1665–1680.
- Reitzer, L.J., and Magasanik, B. (1986). Transcription of *glnA* in *E. coli* is stimulated by activator bound to sites far from the promoter. *Cell* 45, 785–792.
- Rippe, K., Guthold, M., von Hippel, P.H., and Bustamante, C. (1997). Transcriptional activation via DNA-looping: visualization of intermediates in the activation pathway of *E. coli* RNA polymerase- $\sigma$ 54 holoenzyme by scanning force microscopy. *J. Mol. Biol.* 270, 125–138.
- Sasse-Dwight, S., and Gralla, J.D. (1988). Probing the *Escherichia coli glnALG* upstream activation mechanism in vivo. *Proc. Natl. Acad. Sci. U S A* 85, 8934–8938.
- Schulz, A., Langowski, J., and Rippe, K. (2000). The effect of the DNA conformation on the rate of NtrC activated transcription of *Escherichia coli* RNA polymerase- $\sigma$ (54) holoenzyme. *J. Mol. Biol.* 300, 709–725.
- Sexton, T., Yaffe, E., Kenigsberg, E., Bantignies, F., Leblanc, B., Hoichman, M., Parrinello, H., Tanay, A., and Cavalli, G. (2012). Three-dimensional folding and functional organization principles of the *Drosophila* genome. *Cell* 148, 458–472.
- Shaner, N.C., Campbell, R.E., Steinbach, P.A., Giepmans, B.N.G., Palmer, A.E., and Tsien, R.Y. (2004). Improved monomeric red, orange and yellow fluorescent proteins derived from *Discosoma* sp. red fluorescent protein. *Nat. Biotechnol.* 22, 1567–1572.
- Spitz, F. (2016). Gene regulation at a distance: from remote enhancers to 3D regulatory ensembles. *Semin. Cell Dev. Biol.* 57, 57–67.
- Su, W., Porter, S., Kustu, S., and Echols, H. (1990). DNA-looping and enhancer activity: association between DNA-bound NtrC activator and RNA polymerase at the bacterial *glnA* promoter. *Proc. Natl. Acad. Sci. U S A* 87, 5504–5508.
- Wedel, A., Weiss, D.S., Popham, D., Dröge, P., and Kustu, S. (1990). A bacterial enhancer functions to tether a transcriptional activator near a promoter. *Science* 248, 486–490.
- Yan, Y., Leng, F., Finzi, L., and Dunlap, D. (2018). Protein-mediated looping of DNA under tension requires supercoiling. *Nucleic Acids Res.* 46, 2370–2379.
- Zabidi, M.A., and Stark, A. (2016). Regulatory enhancer-core-promoter communication via transcription factors and cofactors. *Trends Genet.* 32, 801–814.
- Zhang, N., Darbari, V.C., Glyde, R., Zhang, X., and Buck, M. (2016). The bacterial enhancer-dependent RNA polymerase. *Biochem. J.* 473, 3741–3753.

## STAR★METHODS

## KEY RESOURCES TABLE

| REAGENT or RESOURCE                                       | SOURCE            | IDENTIFIER      |
|---|-------------------|-----------------|
| Bacterial and Virus Strains                               |                   |                 |
| AH5244  | Hao et al., 2017b | N/A             |
| AH5467  | This paper        | N/A             |
| Recombinant <i>E. coli</i> stains, as shown in Figure S1A | This paper        | N/A             |
| Chemicals, Peptides, and Recombinant Proteins             |                   |                 |
| o-nitrophenyl-β-D-galactopyranoside (ONPG)                | BioVectra         | Cat # 2360      |
| polymyxin B sulfate                                       | Sigma             | Cat # P4932_5MU |
| 2-mercaptoethanol   | Aldrich           | Cat # M6250     |
| isopropyl-β-D-galactopyranoside (IPTG)                    | BioVectra         | Cat # 1882      |

## CONTACT FOR REAGENT AND RESOURCE SHARING

Further information and requests for resources and reagents should be directed to and will be fulfilled by the Lead Contact, Ian Dodd ([ian.dodd@adelaide.edu.au](mailto:ian.dodd@adelaide.edu.au)).

## EXPERIMENTAL MODEL AND SUBJECT DETAILS

## Strain constructions

Strains were constructed using integrating plasmids and recombineering as previously described (Hao et al., 2017a, 2017b, Priest et al., 2014a, 2014b). Reporters were integrated into either AH5244 = MG1655 *rph*<sup>+</sup>  $\Delta$ *lacIZYA glnL(A129T)* (Hao et al., 2017b) or AH5467, which is AH5244 expressing *lacI* from a single-copy integrant of pIT3-SH-*lacI*<sup>+</sup> (Priest et al., 2014b; Figure S1A) at the  $\phi$ HK022 *att* site.

Reporter genes were integrated into the host chromosome at the  $\lambda$  *attB* site (Figure S1B). The *lacZ* gene was *lacZ*<sup>\*</sup>(O2<sup>-</sup>) carrying mutations to reduce RBS activity and to eliminate the *lacO*2 operator (Hao et al., 2014). The *tom* gene is a tdTomato gene (Shaner et al., 2004) modified by silent mutations in the second half to reduce sequence repetition. The promoter fragment was from -36 to +21 of the *E. coli glnAp2* promoter; the enhancer fragment contained NtrC sites 1 and 2 (-98 to -151). The P<sup>-</sup> mutations changed the -24/-12 sequences from TGGCAC/CGCTT to TaaCAC/CaaTT. Spacer DNA between the enhancer/operator/promoter modules was made up of sequences from within the *E. coli* genes *ftsK* (EcoCyc position 932456-936438), *rne* (114410-1143589), *valS* (4479008-4481858) and the phage 186 *K* tail fiber gene to minimize the likelihood of incorporation of cryptic promoters.

The 20 kb NtrC reporter (Figure S1B) was generated by recombineering as described (Hao et al., 2017a) except that the distal E-Oid module was inserted into the gap region between the *moaA* and *ybhK* genes (EcoCyc MG1655: 816,719-816,720).

DNA sequences of manipulated regions were confirmed, except for some of the larger spacers. Sequences are available on request.

## METHOD DETAILS

## Reporter assays

LacZ assays were as described (Priest et al., 2014b). Cultures were grown in microtiter plates in M9 minimal medium ('M9MM' = 1 x M9 salts, 2 mM MgSO<sub>4</sub>, 0.1 mM CaCl<sub>2</sub>, 0.01 mM (NH<sub>4</sub>)<sub>2</sub>Fe(SO<sub>4</sub>)<sub>2</sub>·6H<sub>2</sub>O, 0.4% glycerol [10 x M9 salts = 67.8 g of NaH<sub>2</sub>PO<sub>4</sub>, 30.0 g of KH<sub>2</sub>PO<sub>4</sub>, 10 g NH<sub>4</sub>Cl and 5 g NaCl/L H<sub>2</sub>O]) at 37°C to late log phase. Cultures were added to a combined lysis-assay buffer, with each well of a microtiter plate containing: 50  $\mu$ L culture + M9MM (usually 20  $\mu$ L culture + 30  $\mu$ L M9MM), 150  $\mu$ L TZ8 (100 mM Tris-HCl pH 8.0, 1 mM MgSO<sub>4</sub>, 10 mM KCl), 40  $\mu$ L ONPG (o-nitrophenyl-β-D-galactopyranoside 4 mg/mL in TZ8), 1.9  $\mu$ L 2-mercaptoethanol, 0.95  $\mu$ L polymyxin B (20 mg/mL). The same bacterial cultures (100  $\mu$ L) were used to measure Tom activity, using a VICTOR X5 plate reader (PerkinElmer) equipped with 544/15 nm excitation and 590/20 nm emission filters (PerkinElmer Cat. 1420-503 and 1420-544). The final Tom units were expressed as (culture fluorescence - *tom*<sup>-</sup> culture autofluorescence)/OD<sub>600</sub>. IPTG (isopropyl-β-D-galactopyranoside) was dissolved in diethylformamide.

## Modeling enhancer activation

### The $J$ versus distance relationship

We reanalysed previous measurements of  $J$  obtained from analysis of LacI loop-dependent repression over a range of DNA distances ( $d$ ) in the *E. coli* chromosome (Hao et al., 2017a; Priest et al., 2014a, 2014b) to obtain a family of  $J$  versus DNA  $d$  relationships. We used only direct  $J$  estimates for LacI looping up to  $d = 50300$  bp, and excluded repeated-measurements of the same DNA segment, giving 27 points (Figure S2A). These data were fitted with a power law of the form  $J = \beta \times d^\gamma$ , where  $\beta$  is the  $J$  (nM) at  $d = 0$  and  $\gamma$  is the decay exponent. Linear fits were obtained to  $\log J = \log \beta + \gamma \times \log d$ , with each of 1000 fitting runs made to a set of data points varied randomly according to their standard deviations and the normal distribution, minimizing  $\Sigma((\text{observed } J - \text{expected } J)^2 / \text{sd})$ . The fit to the unvaried data was  $\beta = 1042666$  nM,  $\gamma = -1.1533$  for  $d$  in bp, with the 1000 varied data fits clustering closely around this (Figure S2A). Note that  $J$  values for individual DNA segments can vary substantially from this relationship.

### E-P looping model

Looping of the enhancer (E) to the closed complex (Pc) is treated by a thermodynamic model, where the fraction of time Pc spends in the looped state,  $F_C$ , is determined by  $J_C$  and  $I_C$  (Hao et al., 2017a; Figure S2B; see main text). We imagine that there will be a number of alternative states of the enhancer under our conditions, only some of which are competent for activation. The parameter  $I_C$  takes this fractional activity of the enhancer into account, and is related to the dissociation constant ( $I_C^*$ ) for the active enhancer bound to Pc (Figure S2B). Since the enhancer and promoter DNA sequences, and the concentration and activation of NtrC are fixed in our experiments, we expect  $I_C$  to be constant under our conditions.  $I_C$  is assumed to be independent of  $J_C$  for distances  $\geq 300$  bp.

### Kinetic model for promoter activity

The kinetic model for the promoter (Figure 1F, reproduced in Figure S2C) is simplified in two respects compared to that of Friedman and Gelles (2012). They identified two closed complexes, an unstable closed intermediate and a more stable complex that is competent for activation. Our  $k_c$  and  $k_u$  thus represent the overall rates of conversion between the free promoter and the activation competent closed complex. Friedman and Gelles (2012) also identified a slow rate of decay of the open complex to the closed complex, which we have ignored. However, our scheme adds specific modeling of DNA looping. We note that our model does not deal with the kinetics of DNA looping, essentially assuming that looping equilibrates quickly. It also does not capture possible stabilization of the closed complex by DNA looping or any possible effects of looping on  $k_e$ .

For any particular combination of  $k_c$ ,  $k_u$ ,  $k_{o-\max}$ ,  $k_e$  and  $I_C$ , the activity of the promoter can be calculated from the  $J_C$  value, as shown in Figure S2C. First,  $F_C$  is calculated from  $I_C$  and  $J_C$ . Then  $k_o$  is calculated as  $k_o = k_{o-\max} \times F_C$ . At steady state the rates of gain and loss of each of the three promoter states are equal, allowing calculation of the fraction of time the promoter spends in each state ( $\theta_f$ ,  $\theta_c$ ,  $\theta_o$ ) from the four rates ( $k_c$ ,  $k_u$ ,  $k_o$ ,  $k_e$ ; Figure S2C). Enhancer-dependant promoter activity in initiations per sec,  $a$ , can then be calculated, and converted to enhancer-dependant promoter activity in LacZ units ( $A$ ) based on our measurement in this reporter of 150 units for the  $\lambda pL$  promoter, which is estimated to initiate once per 4.5 s under our conditions (Liang et al., 1999). Background (non-enhancer-dependent) LacZ units ( $bkg$ ) were obtained from measurements of reporters lacking the enhancer (E<sup>-</sup>).

The model was applied to the  $A$  versus  $d$  data (Figure 1B) to generate 1000 E-P variants. To propagate error, each fit used one of the 1000 power laws obtained from the fitting of the  $J$  versus  $d$  data (Figure S2A), and an error-varied set of the  $A$  versus  $d$  data (each  $A$  value was randomly changed according to its SEM,  $n$  and the  $t$ -distribution). For each fit, random initial values of  $k_c$ ,  $k_u$ ,  $k_{o-\max}$ ,  $k_e$  and  $I_C$  were chosen. For each data point,  $J_C$  was calculated from  $d$ , allowing calculation of promoter activity (Figure S2C). The values of  $k_c$ ,  $k_u$ ,  $k_{o-\max}$ ,  $k_e$  and  $I_C$  were modified iteratively in random steps ( $k_c$ ,  $k_{o-\max}$  and  $k_e$  were constrained below  $1 \text{ s}^{-1}$ , and  $k_u$  below  $10 \text{ s}^{-1}$ ), to find values able to best reproduce the error-varied activity data by minimizing  $\Sigma((\text{observed } A - \text{expected } A)^2 / \text{SEM})$ .

While the 1000 different E-P variants gave close fits to the  $A$  versus  $d$  data (Figure 1B), a large range of values and combinations of the five fitted parameters were obtained. However, minimum values of

0.14, 0.12, 0.13  $\text{s}^{-1}$  for  $k_c$ ,  $k_{o-\max}$ , and  $k_e$  were needed to produce sufficient promoter activity.  $I_C$  values ranged from 965-9107 nM.

## Modeling effects of other DNA loops

### Calculation of $J_C$ from promoter activity

Other DNA loops affect enhancer action by changing  $J_C$  for E-Pc looping. We denote the  $J_C$  value in the presence of the other loop as  $J_{C(L)}$ . In order to measure changes in  $J_C$ , we obtain estimates of  $J_C$  and  $J_{C(L)}$  from the observed promoter activities,  $A$  and  $A_{(L)}$  (Figure S3A). The plot of Figure S3A illustrates the dependence of  $A$  on  $J_C$ , derived from the  $A$  versus  $d$  data (above). The plot for a particular E-P variant is shown, however, all 1000 E-P variants fitted to the  $A$  versus  $d$  data show a similar  $A$  versus  $J_C$  relationship.

The derivation in Figure S3A, using equations from Figures S2B and S2C, shows how  $J_C$  (or  $J_{C(L)}$ ) can be obtained for any E-P variant, from the enhancer-dependent promoter activity,  $a$ , obtained from  $A$  (or  $A_{(L)}$ ) as shown, and the five fitted parameters for that variant ( $k_c$ ,  $k_u$ ,  $k_e$ ,  $k_{o-\max}$  and  $I_C$ ).  $J_C$  and  $J_{C(L)}$  values obtained in this way were used in all measurements of the effects of other loops on E-P activity.

### Calculation of $\alpha$ from promoter activity in the presence of a second DNA loop

To quantitate loop assistance and loop interference caused by a nested or alternating LacI loop, we applied a general two-loop model (Figure S2B; Hao et al., 2017a; Priest et al., 2014a). In the model, each individual loop has a weight given by  $J$  for the DNA distance between the sites, and  $I$  for the proteins and sites forming the loop (as in Figure 1D). If each loop forms independently, then the double-looped species has a weight that is the simple product of the two individual weights. Non-independence is quantified by applying  $\alpha$  to the double-loop weight (Priest et al., 2014a).  $\alpha = 1$  means the loops form independently;  $\alpha > 1$  means that the double-looped

species forms more often than expected (loop assistance);  $\alpha < 1$  means that the double-looped species forms less often than expected (loop interference). The double-looped nested species contains two protein bridges and two DNA loops: the internal b loop, and a composite loop of the a and c DNA segments flanked by the protein bridges. Its weight can thus be written as  $(J_b \cdot J_{ac}) / (I_1 \cdot I_2)$ , which gives  $\alpha = J_{ac} / J_{abc}$ .

Figure S3C shows how  $\alpha$  is obtained from reporter measurements in the case of loop assistance. The same process is used for loop interference. Combining equations for the one- and two-loop thermodynamic models, an equation can be derived that expresses  $\alpha$  in terms of the  $J_C$  and  $J_{C(L)}$  values calculated (as described above and in Figure S3A) from the promoter activities in the absence or presence of the other loop, as well as the fractional looping of the other loop,  $F_L$  (Figure S3C). It can be seen that  $\alpha = 1$  when  $J_{C(L)} = J_C$  (no loop interaction),  $\alpha > 1$  when  $J_{C(L)} > J_C$  (loop assistance),  $\alpha < 1$  when  $J_{C(L)} < J_C$  (no loop interaction).

To propagate error, 1000  $\alpha$  values were calculated from any set of loop interaction data. In each calculation, an E-P variant and its associated  $J$  versus  $d$  power law was randomly chosen from the set of 1000 fits to the  $A$  versus  $d$  data. The set of paired observed promoter activities in the absence and presence of the other loop,  $A$  and  $A_{(L)}$ , and the  $E^-$  bkg were error-varied (each value was randomly changed according to its SEM,  $n$  and the  $t$ -distribution), and  $J_C$  and  $J_{C(L)}$  values were calculated according to the parameters of the E-P variant (Figure S1C).  $\alpha$  was calculated from these values and  $F_L$  (Figure S3C), with  $F_L$  for the Oid-O1 LacI loop calculated using  $l_L = 35.0 \pm 3.3$  nM (Hao et al., 2017a; values were error-varied using the 3.3 nM SD and the normal distribution), and  $J_L$  obtained from the relevant  $d$  and the  $J$  versus  $d$  power law of the chosen E-P variant. Negative values for  $\alpha$  can arise if the reduction in  $J_C$  by the insulating loop is greater than could be expected for the estimated strength of the insulating loop ( $J_{C(L)} / J_C + F_L < 1$ ), which can result if the insulating loop strength is underestimated.

### Modeling of promoter competition

Figure S4A shows the model for how sequestration of the enhancer by P2 reduces looping of the enhancer to the closed complex at P1. Looping to closed and open complexes was allowed. The sequestration can be quantitated as a change in  $J$ , with an effective  $J_{C1(2)}$  for E-Pc1 in the presence of P2.

For Figure 5B, this model was used to calculate the expected ratio of the activity of P1 in the presence or absence of P2 for a given set of the five E-P parameters ( $k_c$ ,  $k_u$ ,  $k_e$ ,  $k_{o-max}$  and  $I_C$ ). Expected enhancer-dependent activity in the absence of P2,  $a_{P1}$ , was calculated as above (Figure S2C), using  $J_{C1}$  from the  $J$  versus  $d$  relationship. Expected values for  $J_{C1(2)}$  were then obtained according to the equation in Figure S4A, from  $J_2$  for the E-P2 segment (from the  $J$  versus  $d$  relationship) and the fractional occupation of the closed and open complex states at P2,  $\theta_{2c}$  and  $\theta_{2o}$  (calculated as for P1 from  $k_c$ ,  $k_u$ ,  $k_e$ ,  $k_{o-max}$  and  $I_C$ ; Figure S2C). Since competition is reciprocal, and the presence of P1 also affects E-P2 looping, the same analysis was applied to P2 using the  $\theta_{1c}$  and  $\theta_{1o}$  values based on the calculated  $F_{1(2)}$ . This produced an  $F_{2(1)}$  value and new  $\theta_{2c}$  and  $\theta_{2o}$  values. This reciprocal competition calculation was iterated until the values of  $\theta_{1c}$ ,  $\theta_{1o}$ ,  $\theta_{2c}$  and  $\theta_{2o}$  changed minimally between iterations. The stable  $F_{1(2)}$  value was used to calculate the expected activity of P1 in the presence of P2,  $a_{P1(P2)}$ .

To fit the data in Figure 5B, fixed values for  $I_C = 10, 100, 1000, 5000$  or  $10000$  nM were used and values of  $k_c$ ,  $k_u$ ,  $k_e$ ,  $k_{o-max}$  were modified by a Monte-Carlo procedure to find expected  $a_{P1(P2)} / a_{P1}$  ratios that best matched the observed ratios in the competition data by minimizing  $\Sigma((observed\ ratio - expected\ ratio)^2 / SEM)$ , and that also produced  $A_{P1} = 6.8$  LacZ units (for E-P1 3500 bp).

### Modeling of enhancer additivity

Each enhancer combines to increase the effective enhancer concentration seen by the closed complex, thus increasing  $J_C$  (Figure S6C). For each additional enhancer, a similar term is added to the equation for  $J_{C(E12)}$ . For the case of enhancers where the interaction strength of the enhancers with Pc is the same ( $I_{C1} = I_{C2}$ ), then  $J_{C(E12)}$  is simply the sum of the  $J_C$  values for each enhancer. Note that this analysis assumes that  $k_{o-max}$  is the same for the different enhancers. In reality, different enhancers may have different effects on  $k_o$  (i.e.,  $k_{o-max}$  may differ) and so could affect activation differently.

## QUANTIFICATION AND STATISTICAL ANALYSIS

Reported LacZ and Tom units are generally obtained from assays of three separate colonies of the particular strain performed on three separate days ( $n = 9$ ). Average values are given  $\pm$  95% confidence limits calculated using the  $t$ -distribution.

Fold regulation is calculated as the ratio of the Oid<sup>+</sup>O1<sup>+</sup> and Oid<sup>-</sup>O1<sup>+</sup> units after subtraction of the  $E^-$  LacZ background or the P<sup>-</sup> Tom background. Final errors are obtained by error propagation, including the error in the background.

For the promoter competition data (Figure 5A), 15 measurements P1 in the presence of P2 or in the absence of P2 ( $E^-$  backgrounds subtracted) were paired and individual ratios calculated. The mean and 95% confidence limits ( $t$ -distribution) were calculated using logs of the 15 ratios.